Supplementary Materials

Atomistic to Mesoscopic Modelling of Thermophysical Properties of Graphene-Reinforced Epoxy Nanocomposites

Supplementary Note S1: Crosslinking mechanism

i. Atomistic model of epoxy

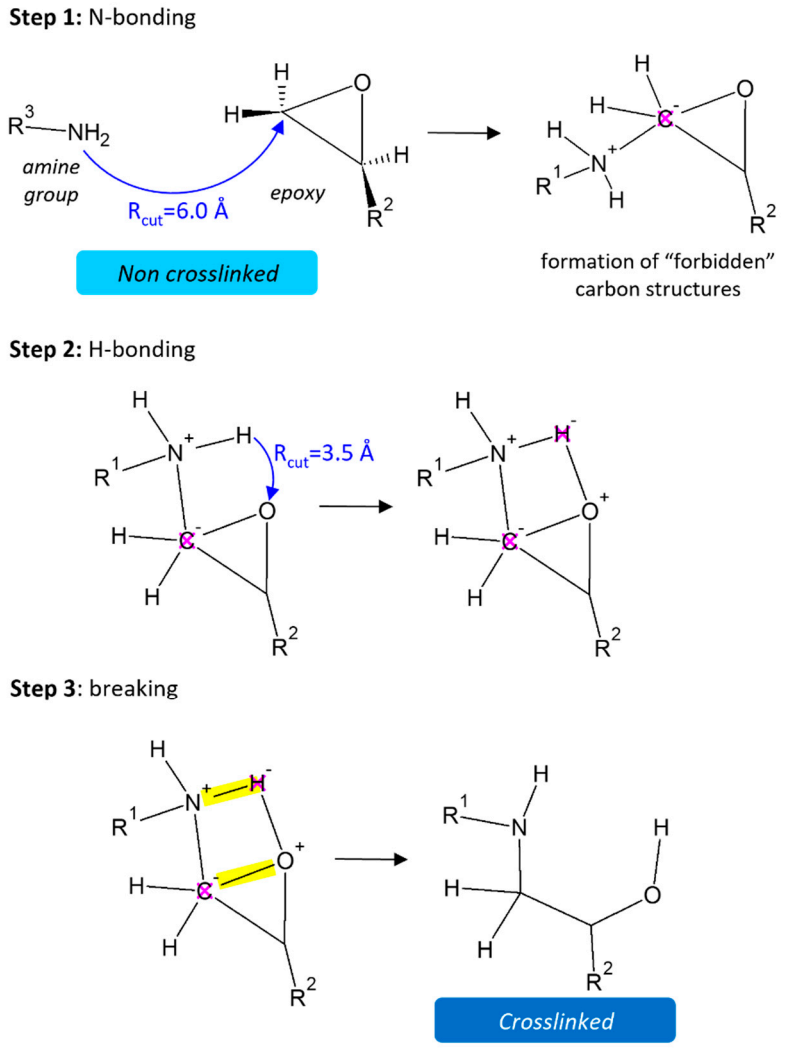

Figure S1. Cross-linking protocol for hardeners containing amine groups.

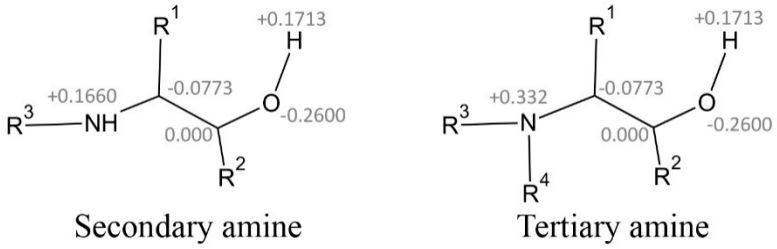

Figure S2. Charge update (Δq) of atoms after cross-linking process (values in eV).

ii. Mesoscopic model of epoxy

Polymer	Type of bead	Bead ID*	Description of bead
Epoxy resin (EPO)	E	1	Beads containing unreacted epoxy group in DGEBA
	G	2	Oxyphenylene groups in DGEBA
	B	3	Bead containing central dimethyl group in DGEBA
	Ad	4	Primary amine group in DETA
	Ae	5	Secondary amine group in DETA
	Ay	6	Amine group in DICY
	Y	7	Non-amine group in DICY
	E’	8	Beads containing reacted epoxy group in DGEBA
	Ad1	9	Primary amine group in DETA – reacted once
	Ad2	10	Primary amine group in DETA – reacted twice
	Ae1	11	Secondary amine group in DETA – reacted
	Ay1	12	Amine group in DICY – reacted once
	Ay2	13	Amine group in DICY – reacted twice

Table S1. List of beads for coarse-grained (CG) model of epoxy resin.

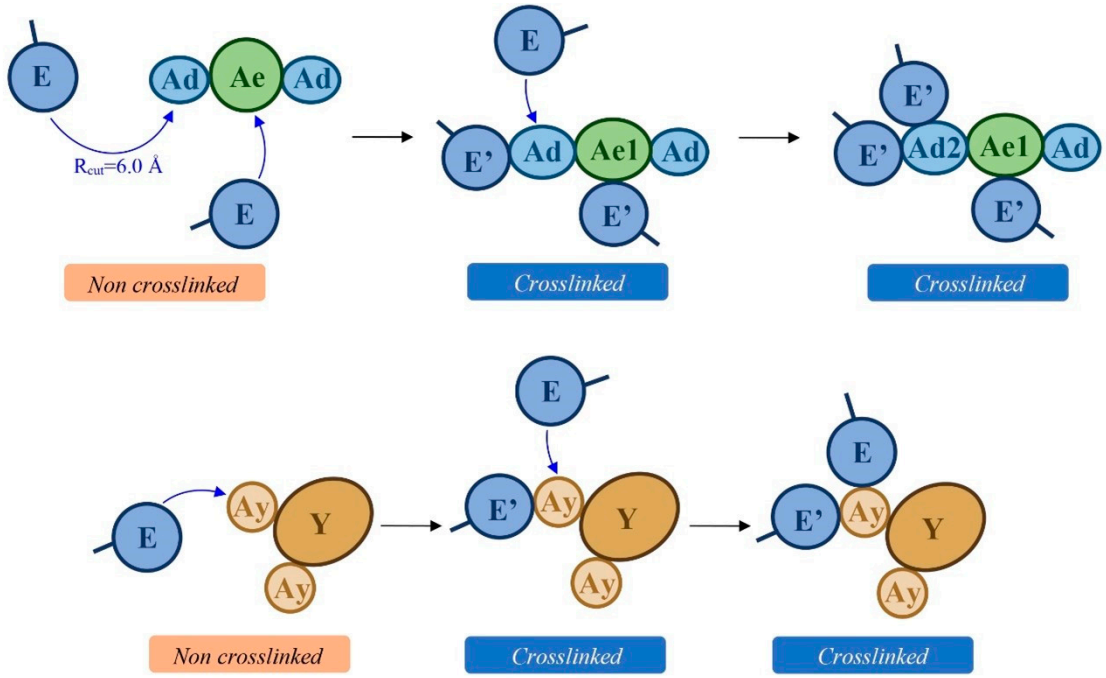

Figure S3. Cross-linking mechanism of CG beads.

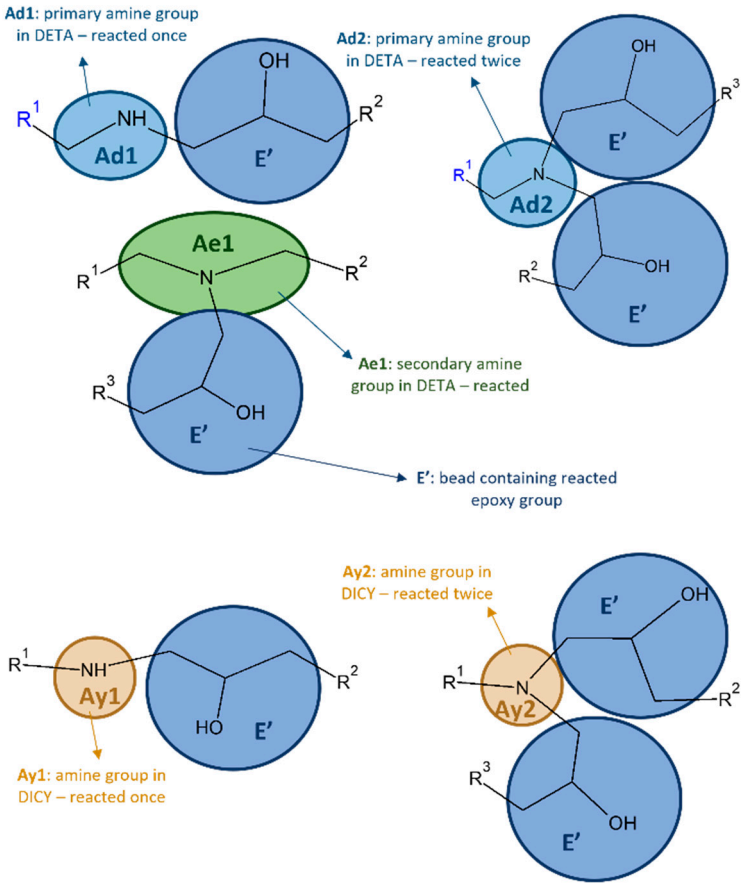

Figure S4. Mapping scheme for cross-linked groups of epoxy resin.

Supplementary Note S2: Mesoscopic model of graphene

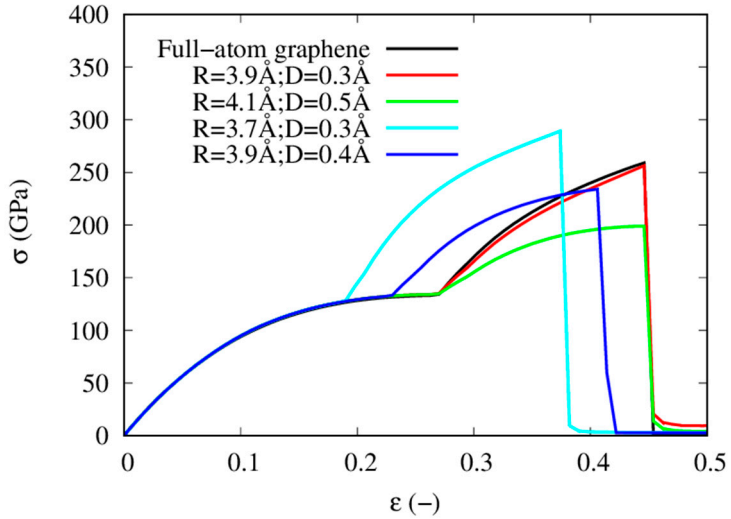

Figure S5. Optimization of the values of R and D for the TersoffCG potential.

Parameter	Tersoff potential	TersoffCG potential
m	3	3
γ	1	1
$\lambda_3(\text{Å}^{-1})$	0	0
c	38049	38049
d	4.3484	4.3484
$\cos\theta_0$	-0.57058	-0.57058
n	0.72751	0.72751
β	0.00000015724	0.00000015724
$\lambda_2(\text{Å}^{-1})$	2.2119	1.10595
B(kcal/mol)	7995.2	31980.8
$R(\text{Å})$	1.95	3.90
$D(\text{Å})$	0.15	0.30
$\lambda_1(\text{Å}^{-1})$	3.4879	1.74395
A(kcal/mol)	32137.67024	128550.68096

Table S2. Parameters of Tersoff and TersoffCG potentials for graphene.

Supplementary Note S3: Epoxy resin CG force field (EPO-CGff)

Bond	Angle			
E – G	E – G – B	E’ – Ae1 – Ad1	E’ – G – B	Ad – Ae1 – Ad2
G – B	G – B – G	E’ – Ae1 – Ad2	Ay2 – Y – Ay	Ad1 – Ae – Ad
Ad – Ae	AY – Y – Ay	G – E’ – Ad1	Ay1 – Y – Ay	Ad2 – Ae1 – Ad2
Ay – Y	Ad – Ae – Ad	G – E’ – Ad2	Ay1 – Y – Ay1	Ad – Ae – Ad2
E’ – Ad1	E’ – Ad1 – Ae	G – E’ – Ae1	Ay1 – Y – Ay2	Ad1 – Ae1 – Ad2
E’ – Ad2	E’ – Ad1 – Ae1	E’ – Ay1 – Y	Ay2 – Y – Ay2	Ad2 – Ae – Ad1
E’ – Ae1	E’ – Ad2 – Ae	E’ – Ay2 – Y	E’ – Ad2 – E’	Ad – Ae1 – Ad1
E’ – Ay1	E’ – Ad2 – Ae1	G – E’ – Ay1	E’ – Ay2 – E’	Ad2 – Ae – Ad2
E’ – Ay2	E’ – Ae1 – Ad	G – E’ – Ay2	Ad – Ae1 – Ad	

Table S3. List of potentials in the developed EPO-CGff force field for bonded interactions (bonds and angles).

Non-bonded				
E ··· E	E ··· Y	G ··· Y	Ad ··· Ad	Ae ··· Y
E ··· G	G ··· G	B ··· B	Ad ··· Ae	Ay ··· Ay
E ··· B	G ··· B	B ··· Ad	Ad ··· Ay	Ay ··· Y
E ··· Ad	G ··· Ad	B ··· Ae	Ad ··· Y	Y ··· Y
E ··· Ae	G ··· Ae	B ··· Ay	Ae ··· Ae	
E ··· Ay	G ··· Ay	B ··· Y	Ae ··· Ay	

Table S4. List of potentials in the developed EPO-CGff force field for non-bonded interactions.

i. Bond potentials

Bond	Potential
E – G	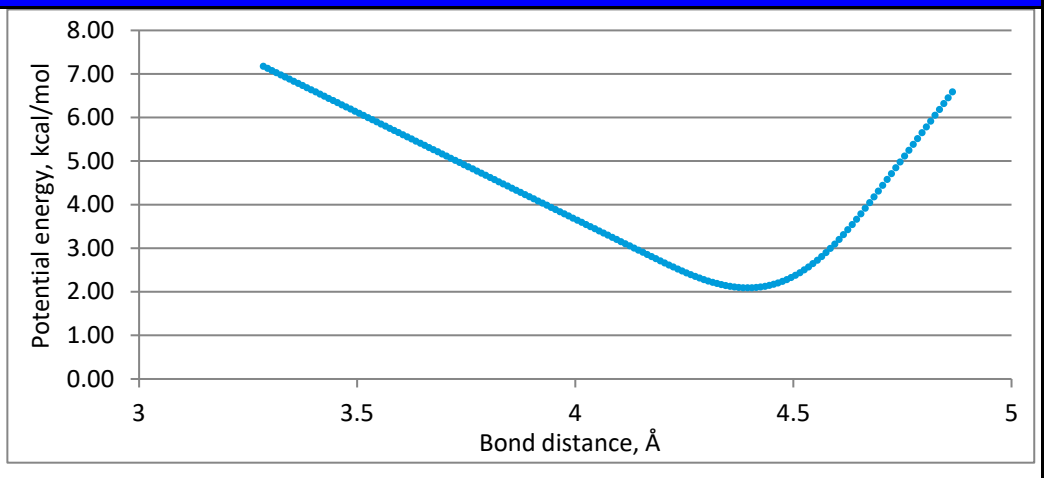

Bond	Potential
G – B	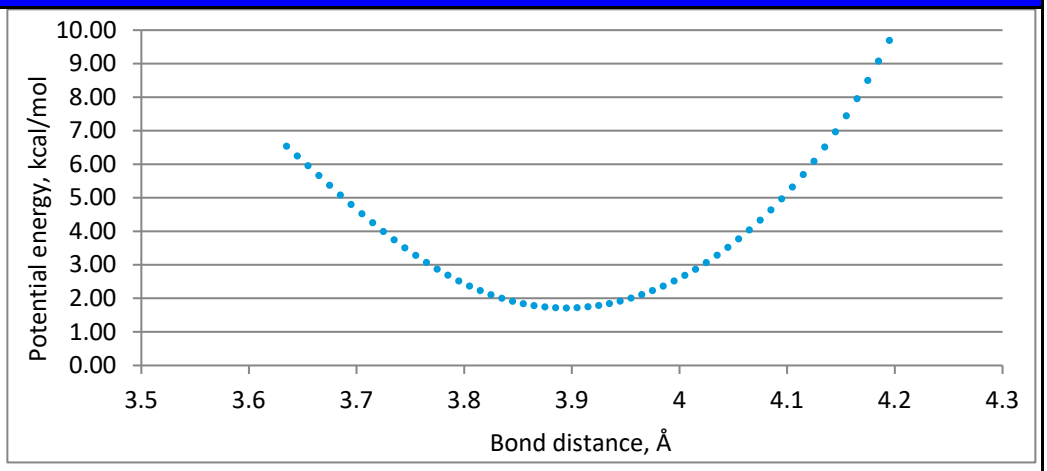
Ad – Ae	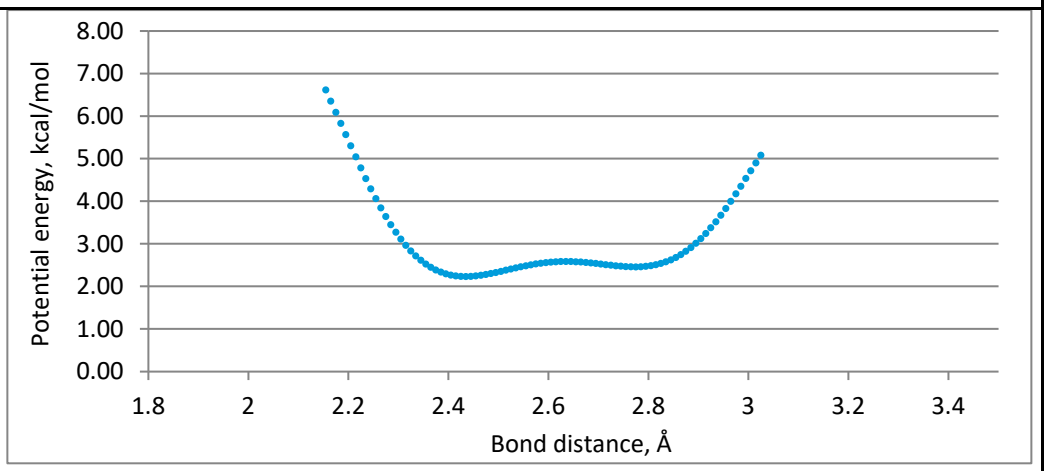
Ay – Y	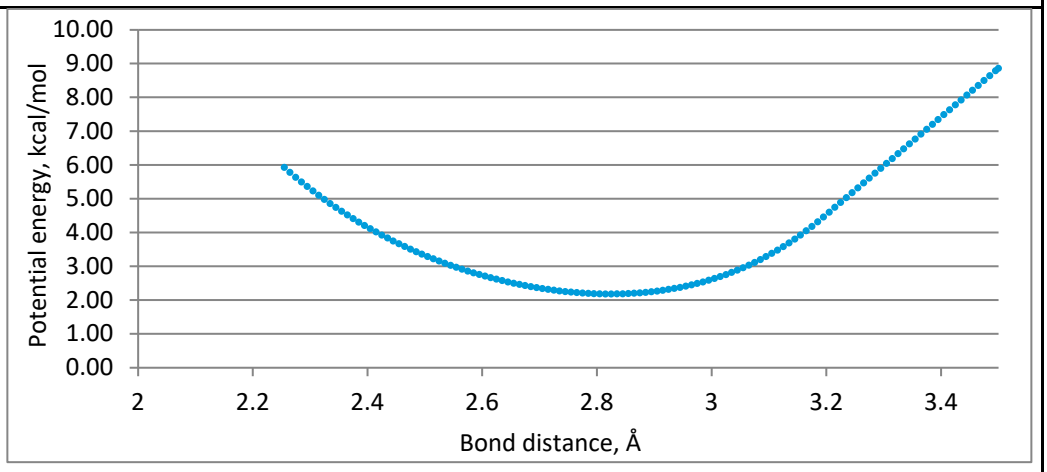

Bond	Potential
E' – Ad1	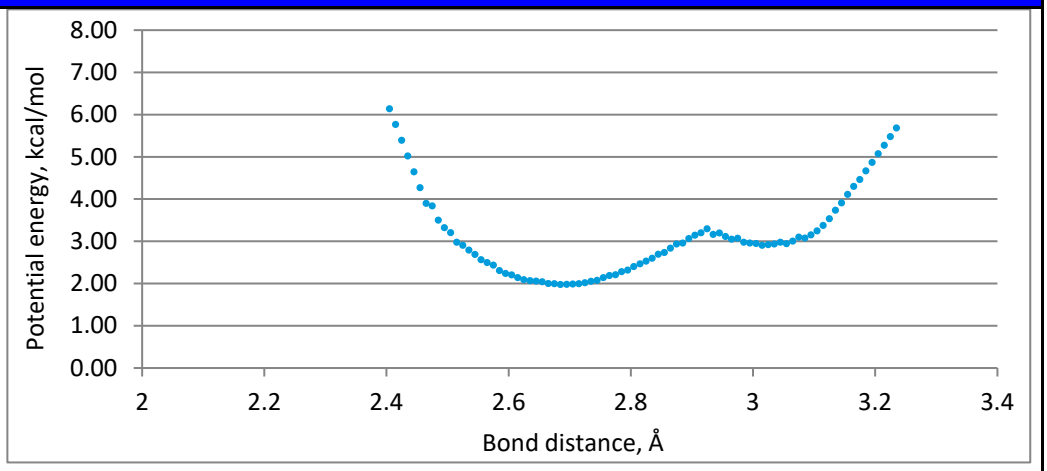
E' – Ad2	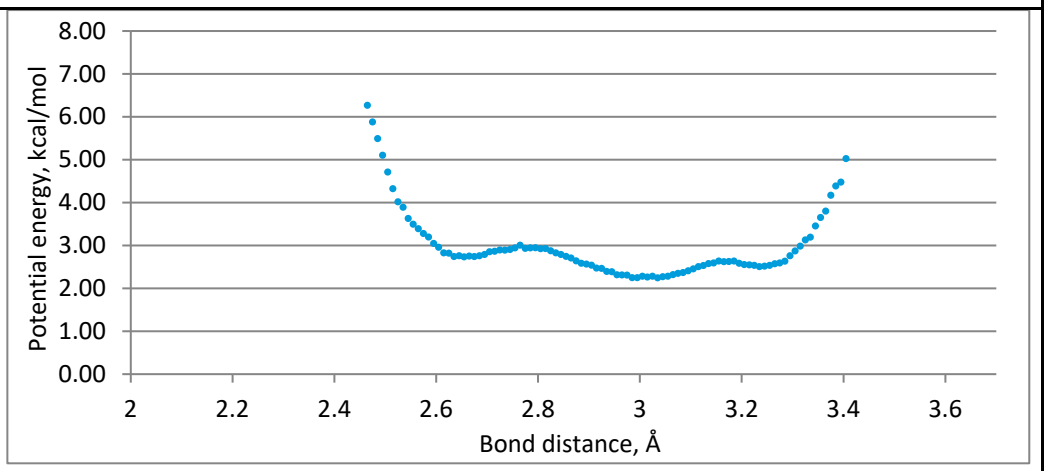
E' – Ae1	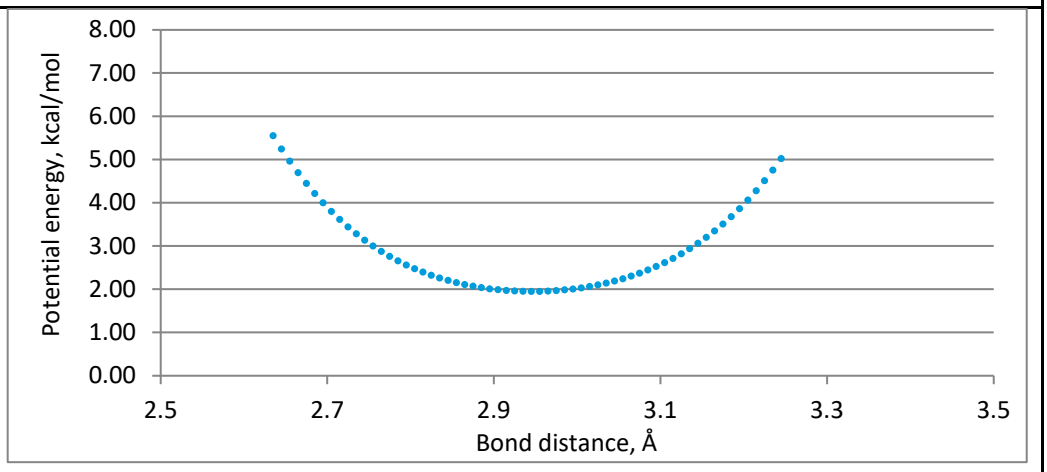

Bond	Potential
E' – Ay1	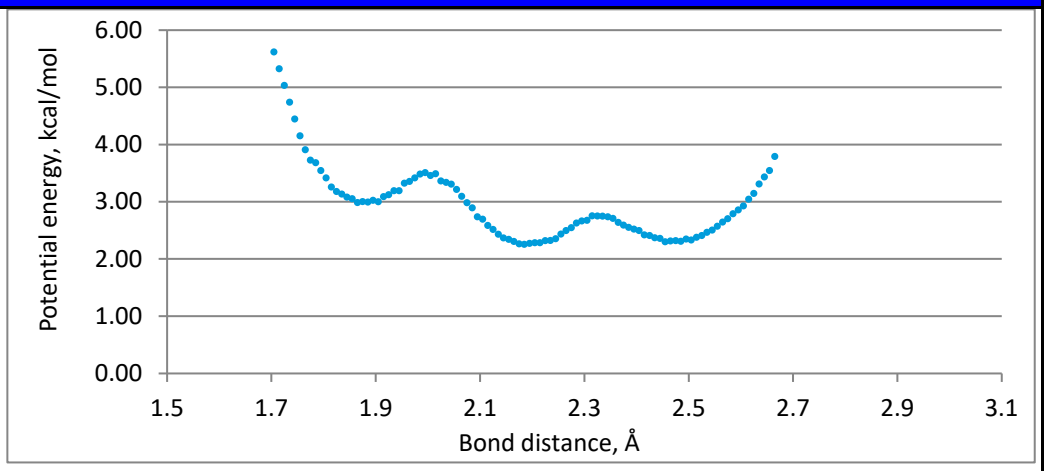
E' – Ay2	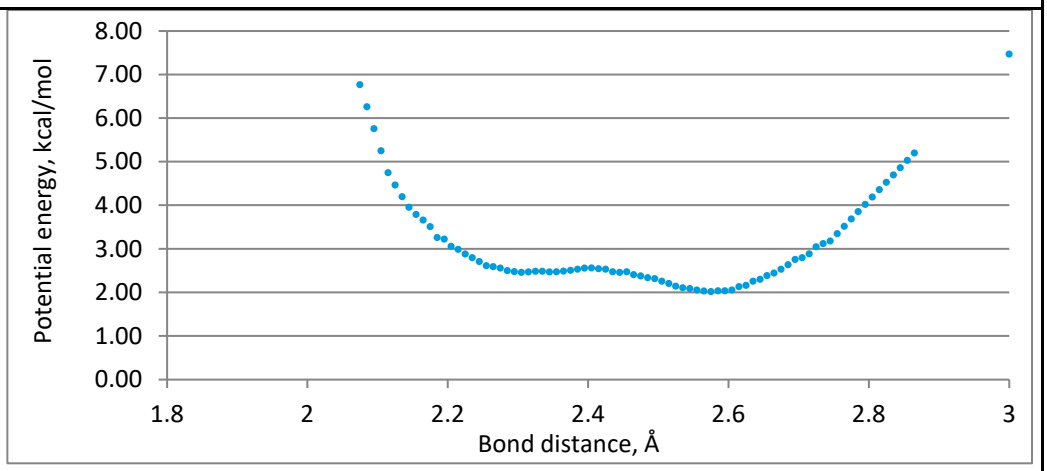

ii. Angle Potentials

Angle	Potential
E – G – B	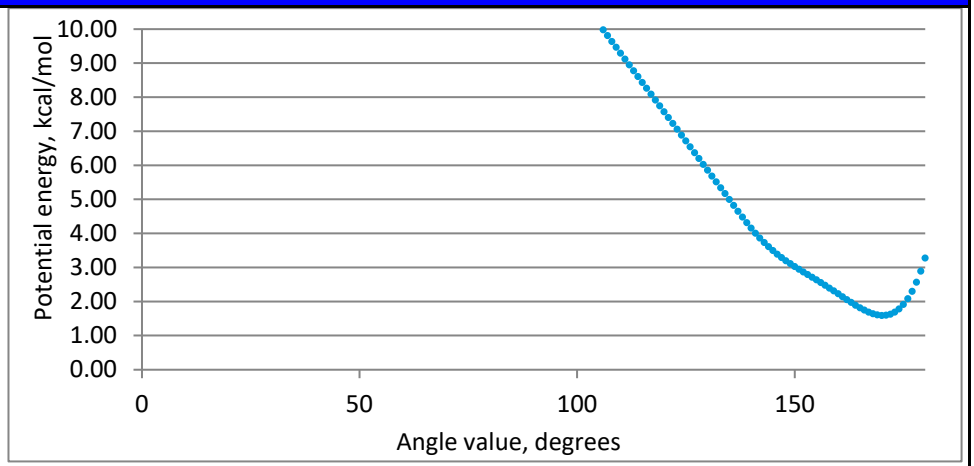

Angle	Potential
G – B – G	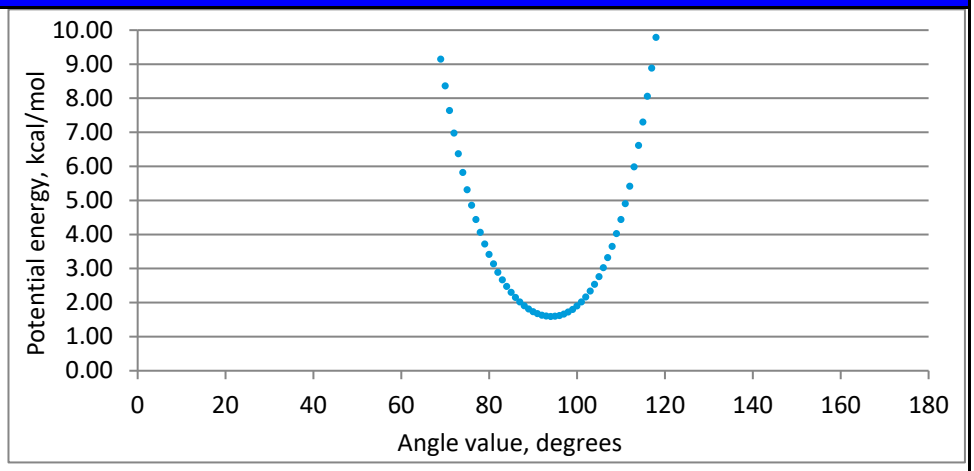
AY – Y – Ay	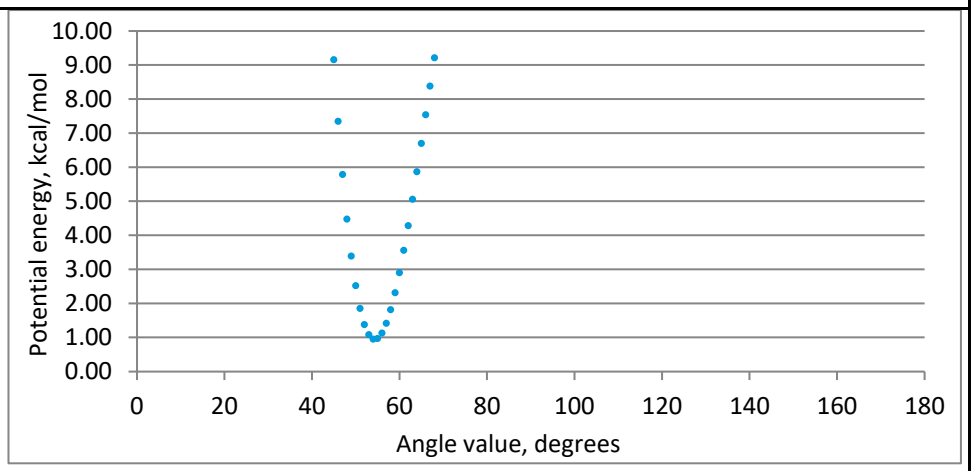
Ad – Ae – Ad	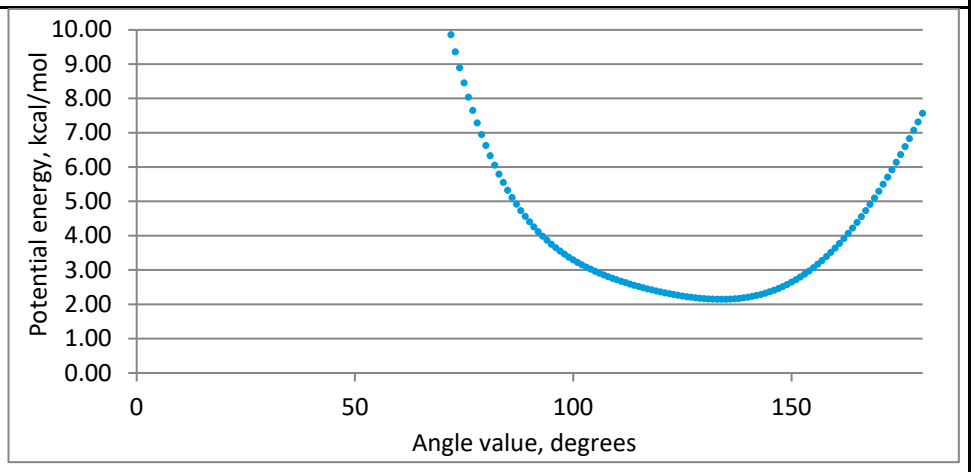

Angle	Potential
E' – Ad1 – Ae	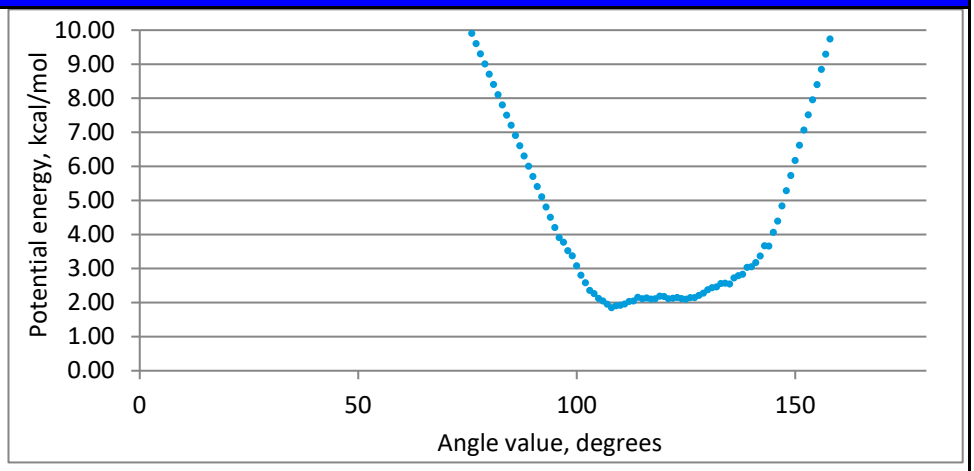
E' – Ad1 – Ae1	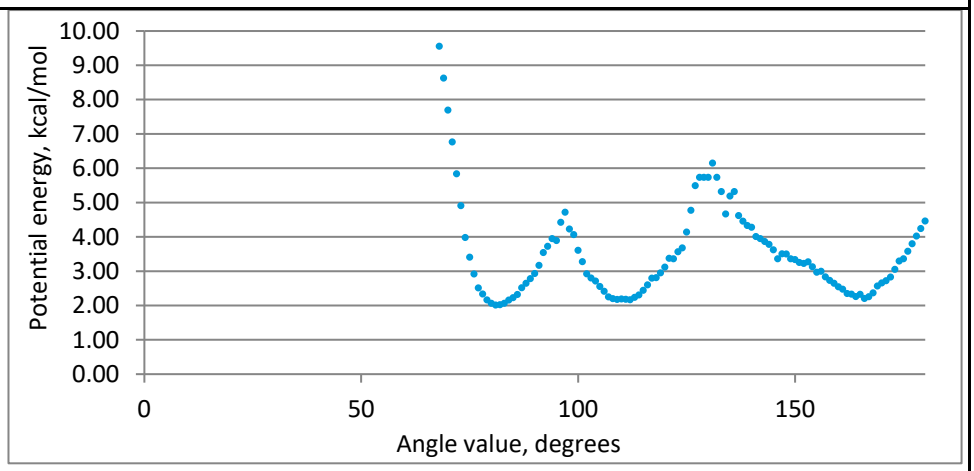
E' – Ad2 – Ae	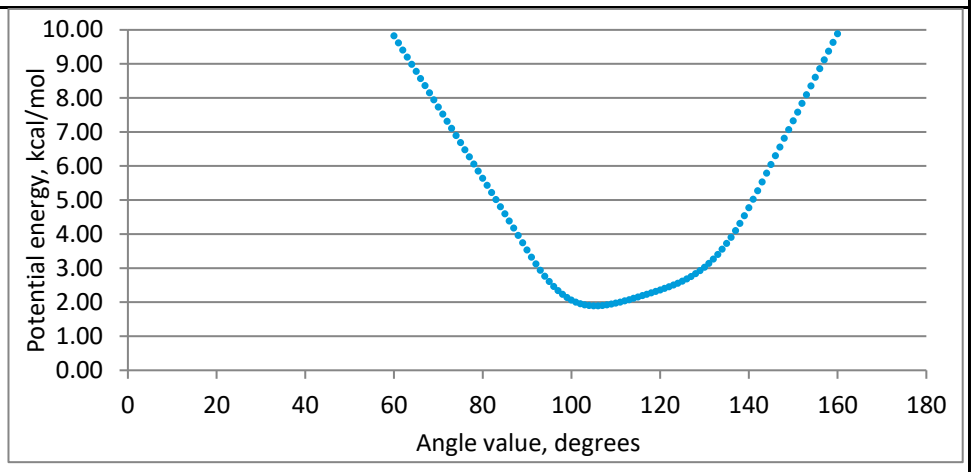

Angle	Potential
E' – Ad2 – Ae1	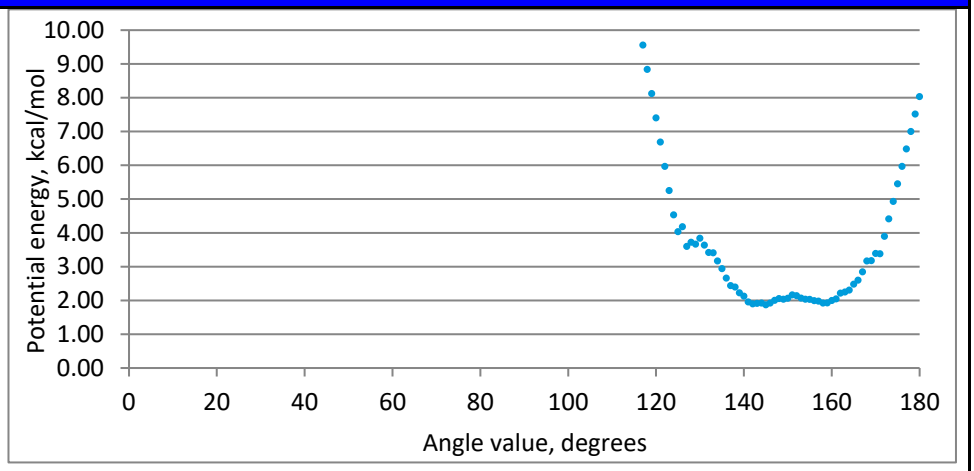
E' – Ae1 – Ad	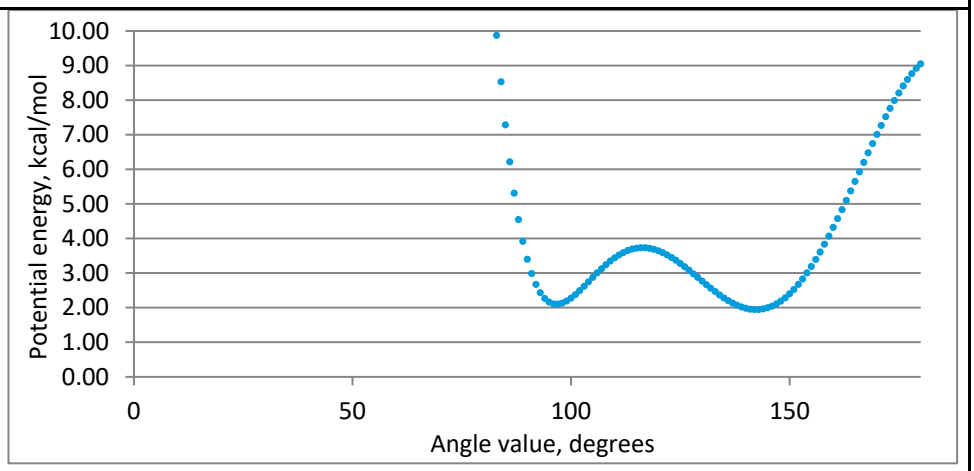
E' – Ae1 – Ad1	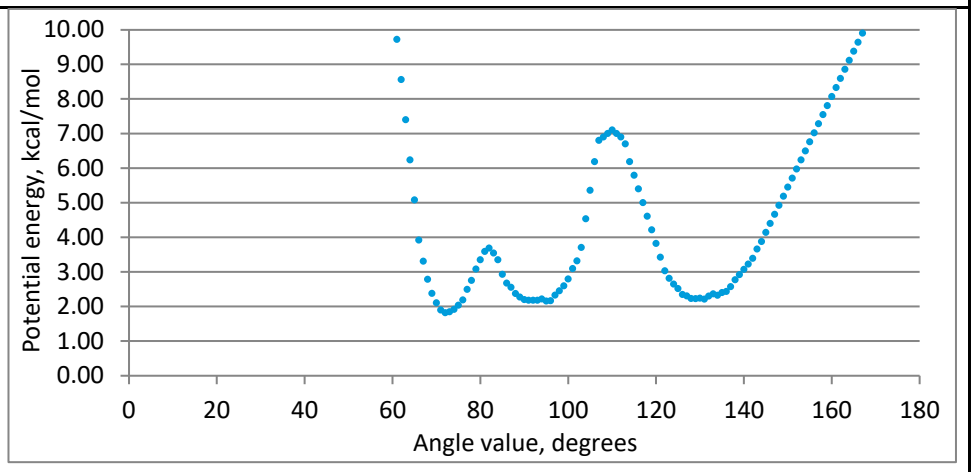

Angle	Potential
E' – Ae1 – Ad2	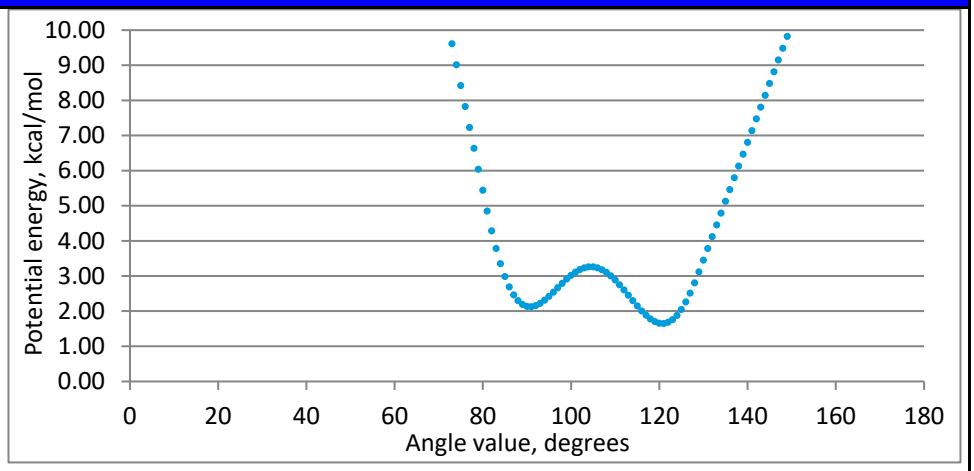
G – E' – Ad1	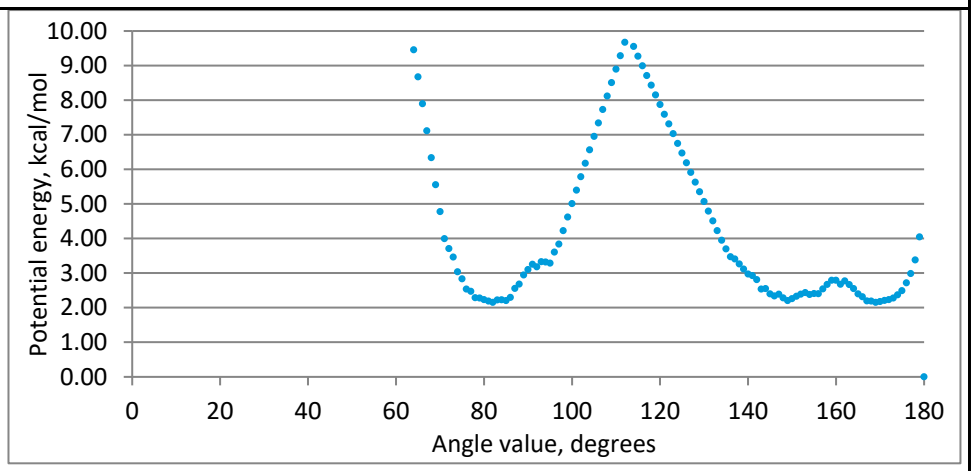
G – E' – Ad2	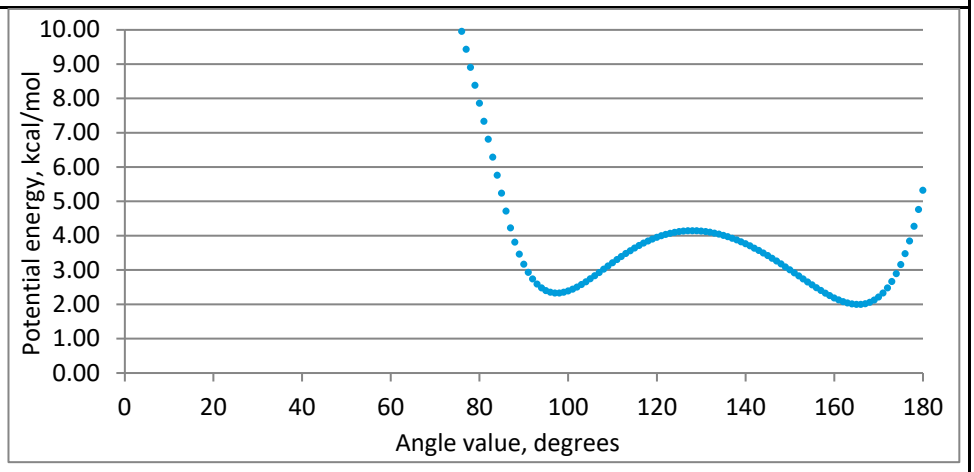

Angle	Potential
G – E' – Ae1	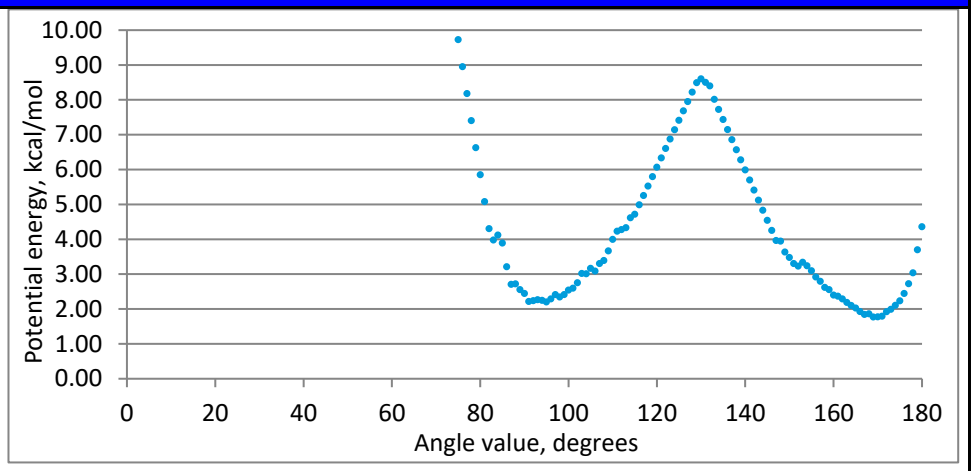
E' – Ay1 – Y	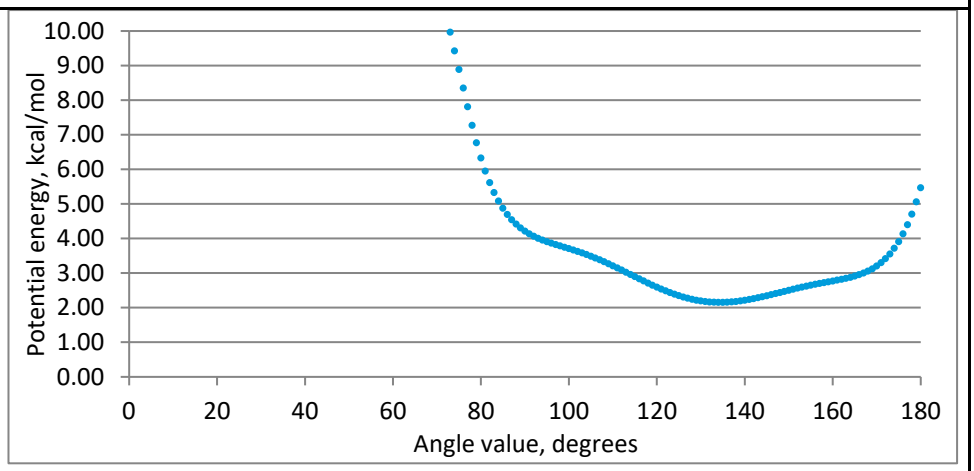
E' – Ay2 – Y	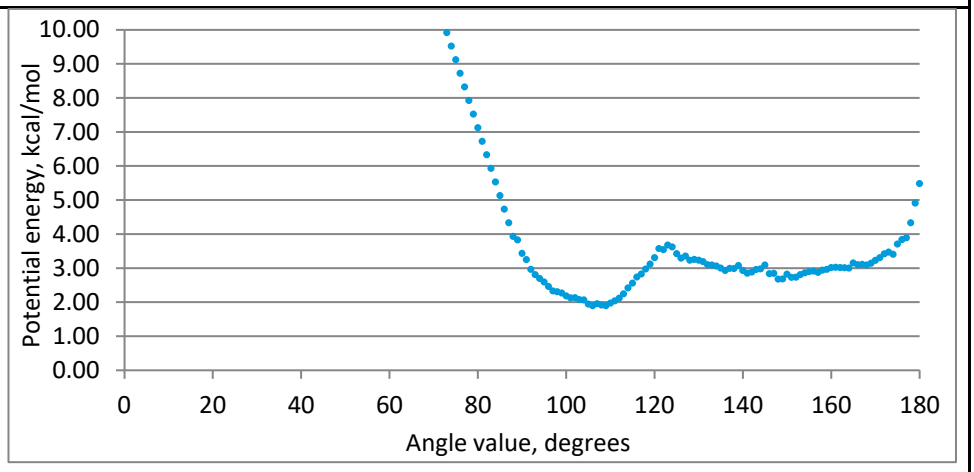

Angle	Potential
G – E’ – Ay1	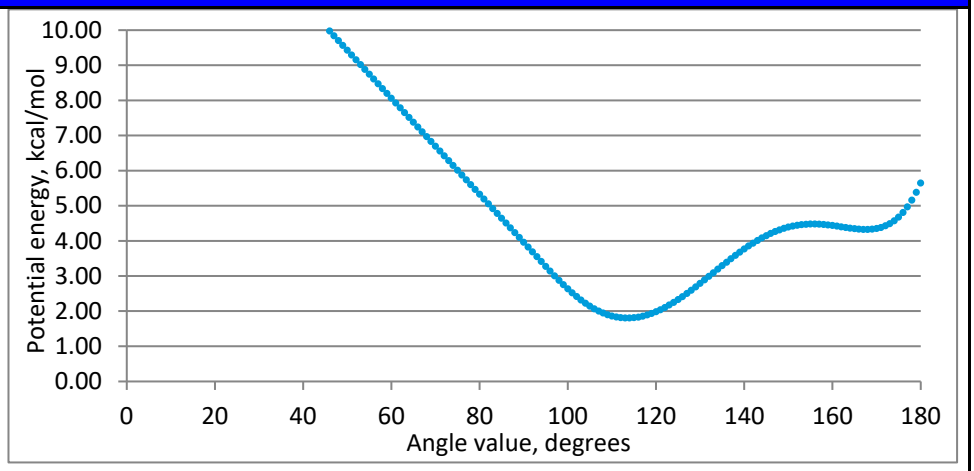
G – E’ – Ay2	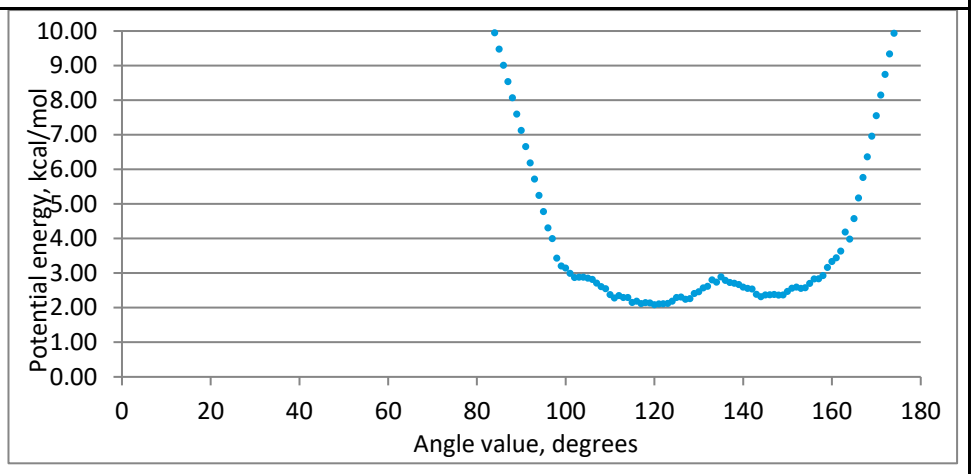
E’ – G – B	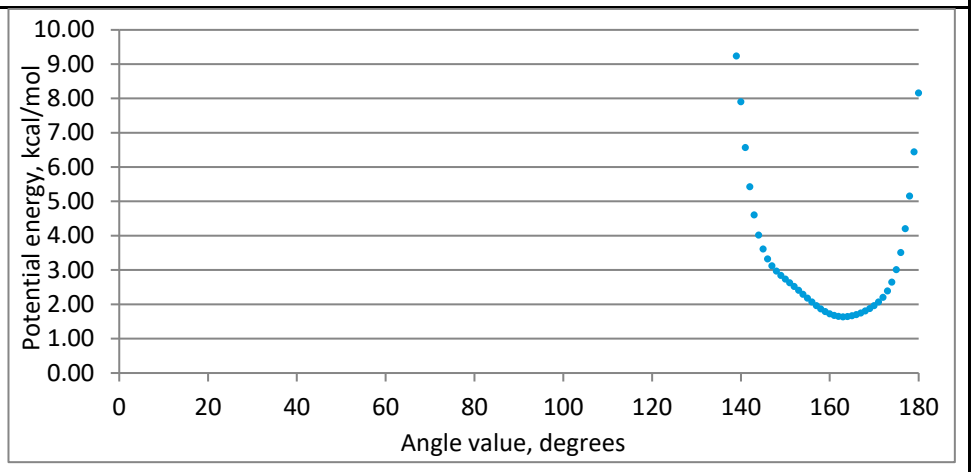

Angle	Potential
Ay2 – Y – Ay	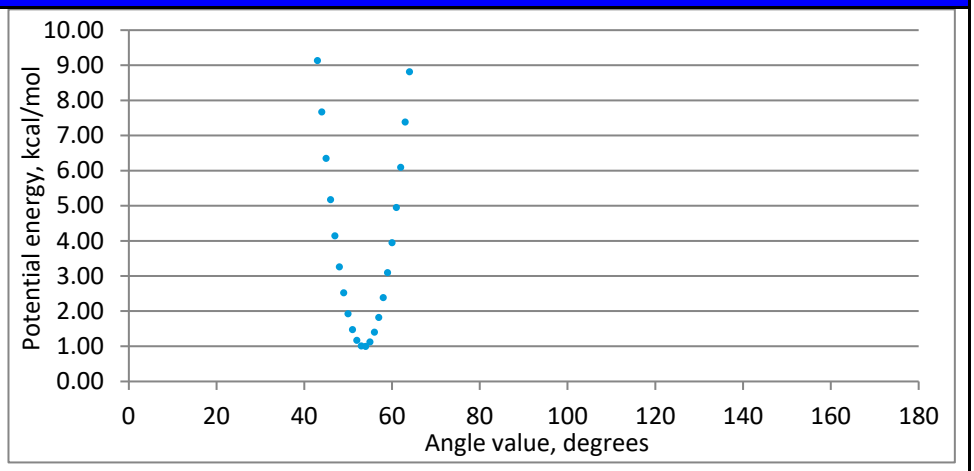
Ay1 – Y – Ay	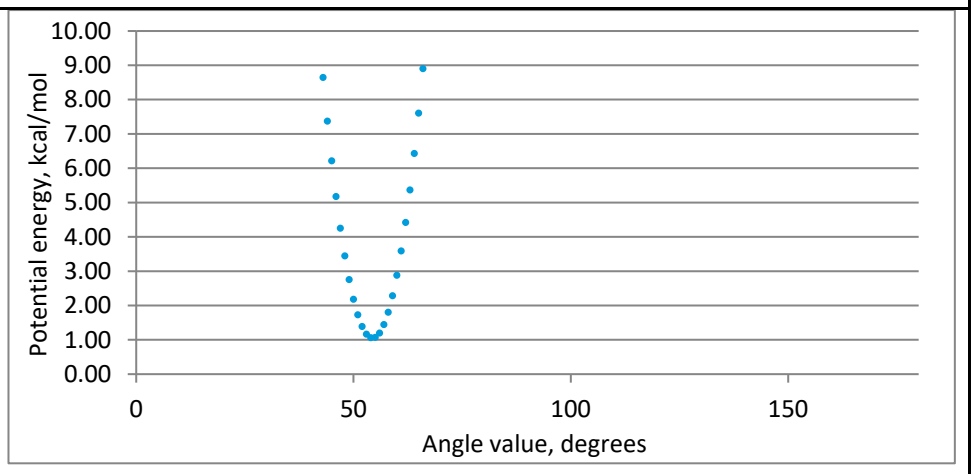
Ay1 – Y – Ay1	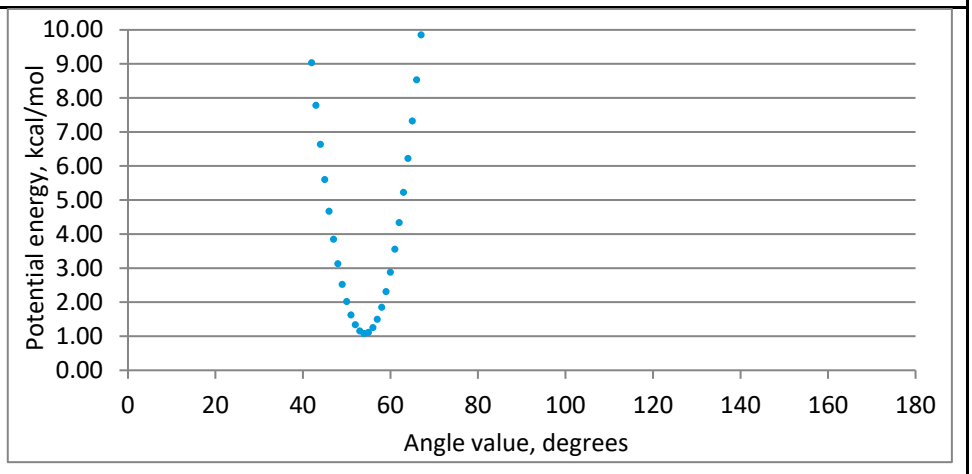

Angle	Potential
Ay1 – Y – Ay2	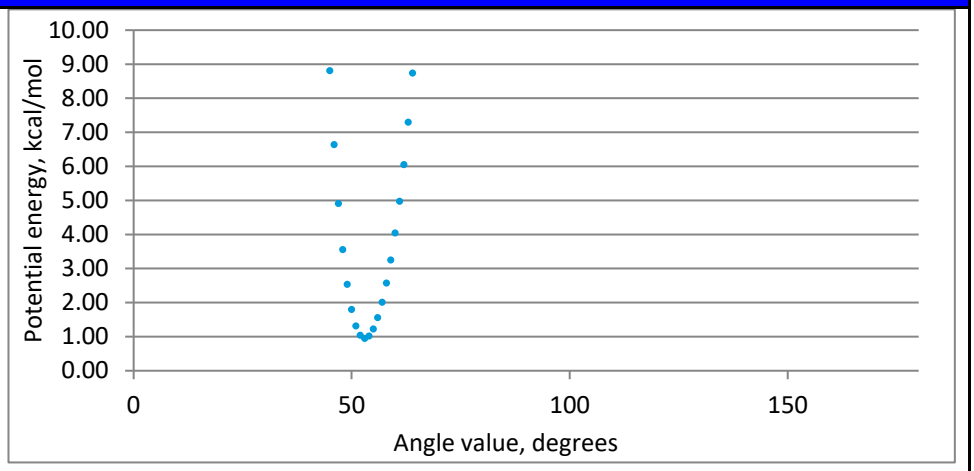
Ay2 – Y – Ay2	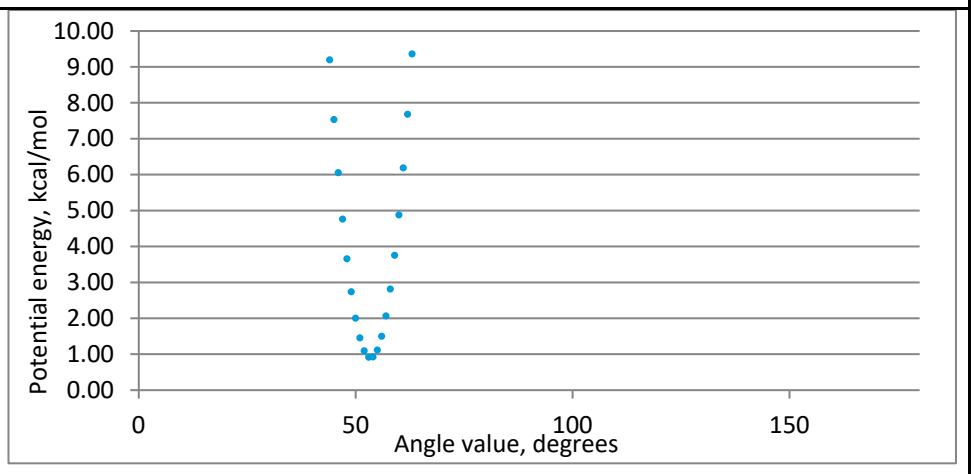
E' – Ad2 – E'	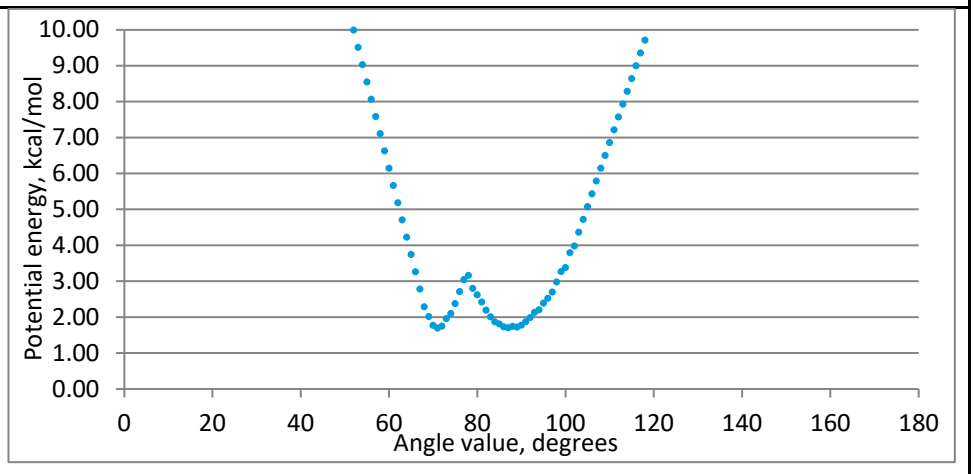

Angle	Potential
E' – Ay2 – E'	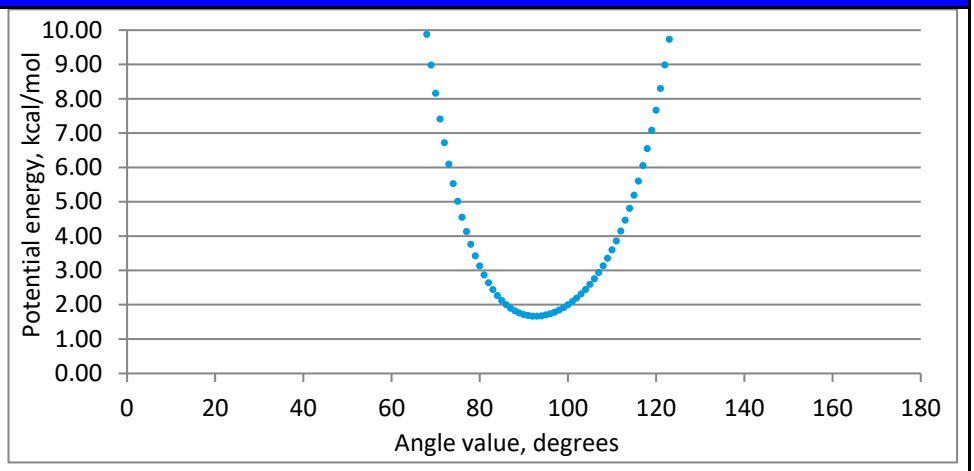
Ad – Ae1 – Ad	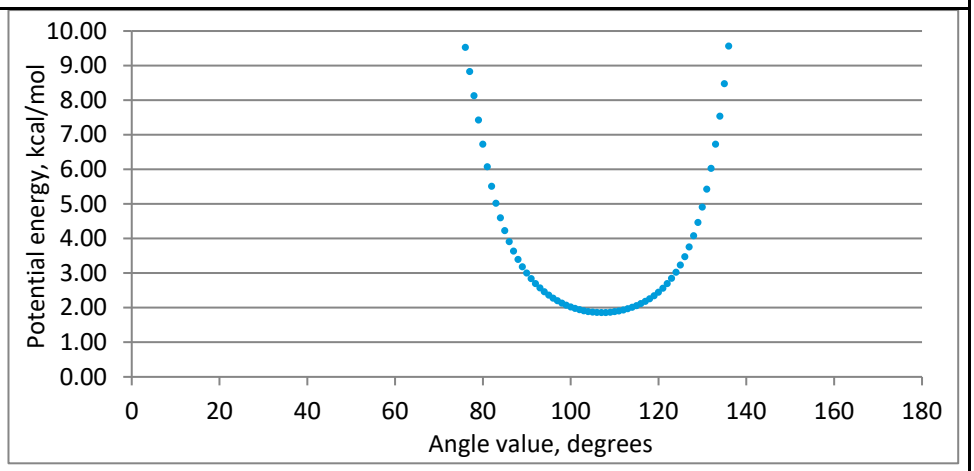
Ad – Ae1 – Ad2	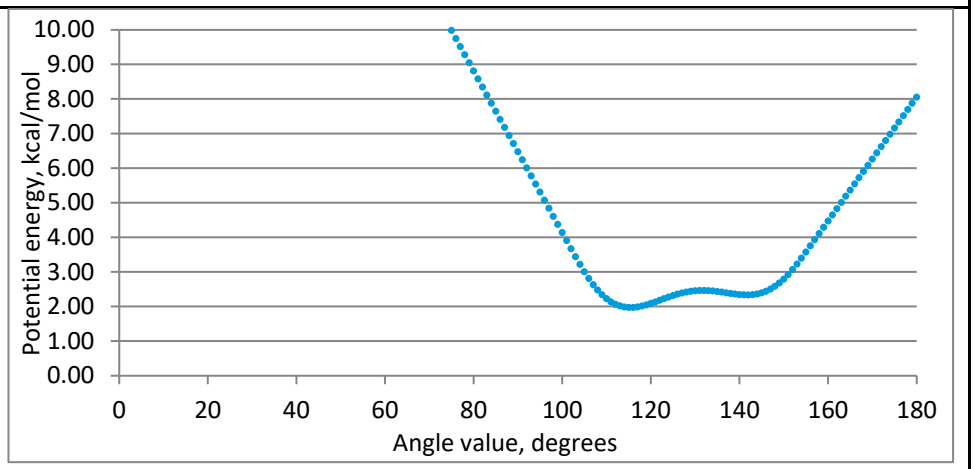

Angle	Potential
Ad1 – Ae – Ad	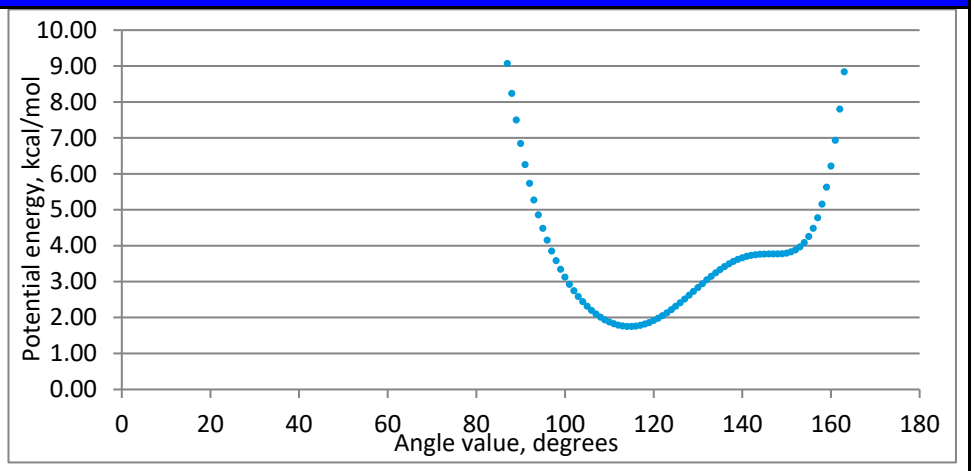
Ad2 – Ae1 – Ad2	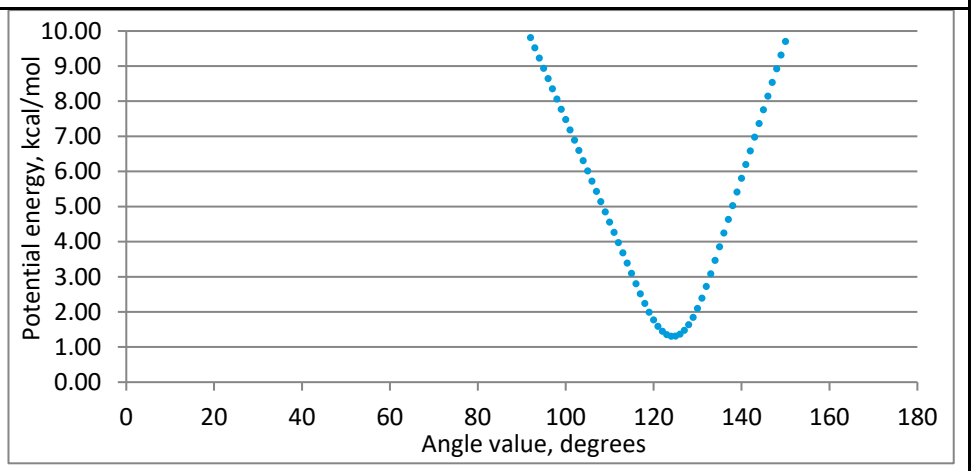
Ad – Ae – Ad2	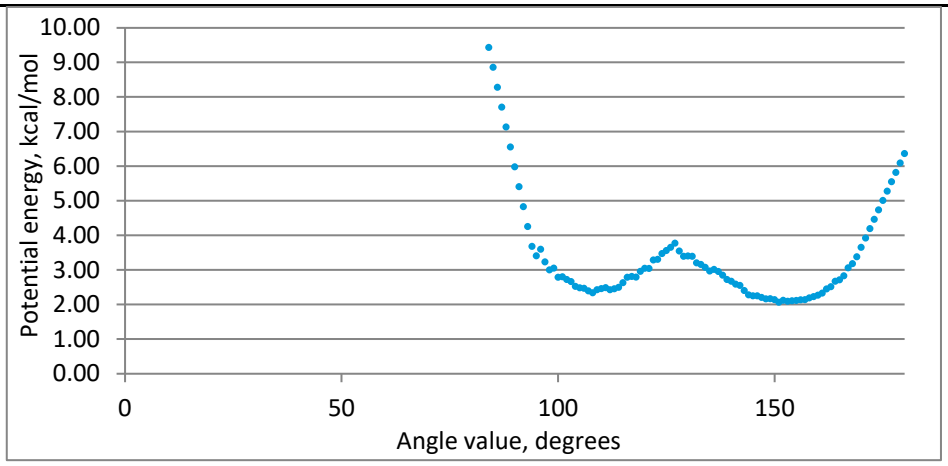

Angle	Potential
Ad1 – Ae1 – Ad2	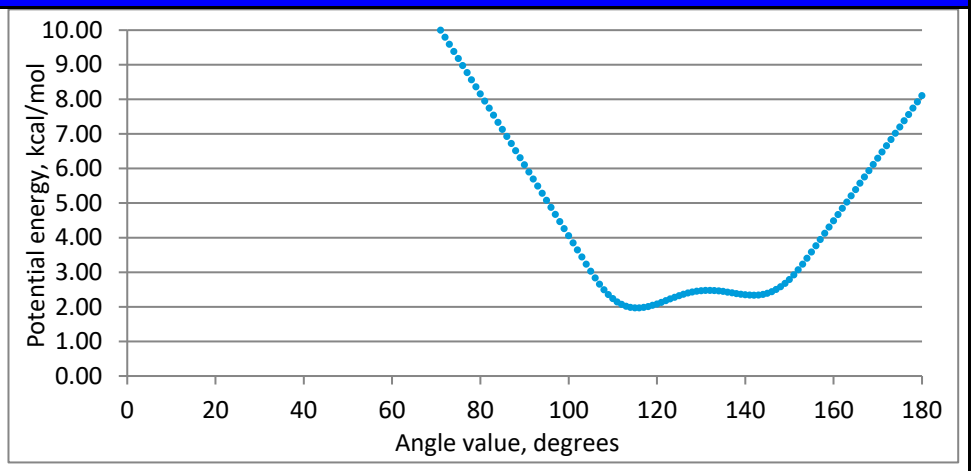
Ad2 – Ae – Ad1	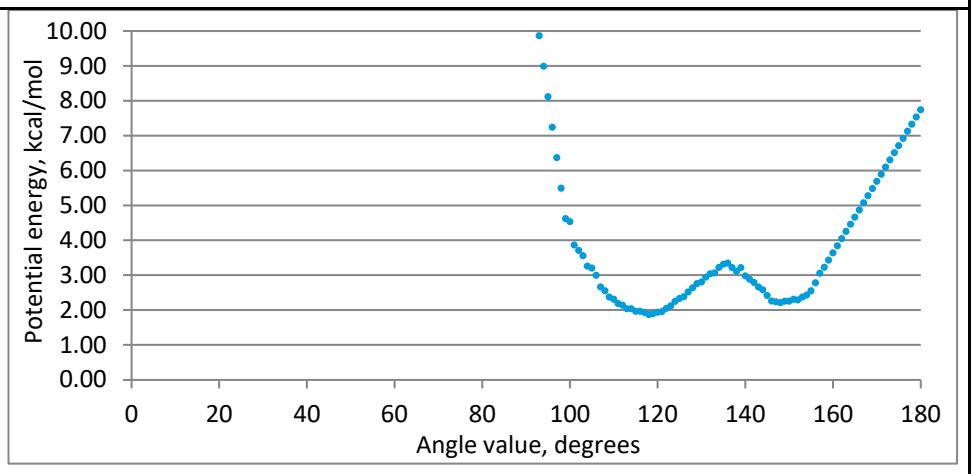
Ad – Ae1 – Ad1	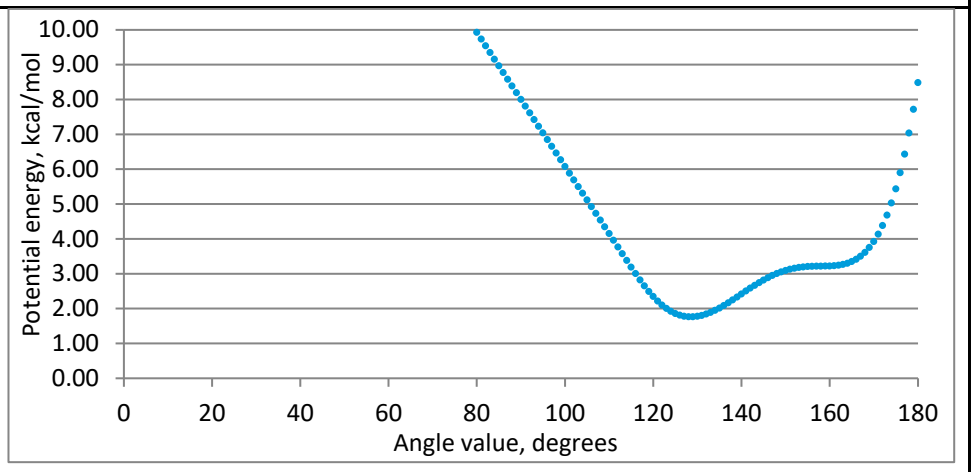

Angle	Potential
Ad2 – Ae – Ad2	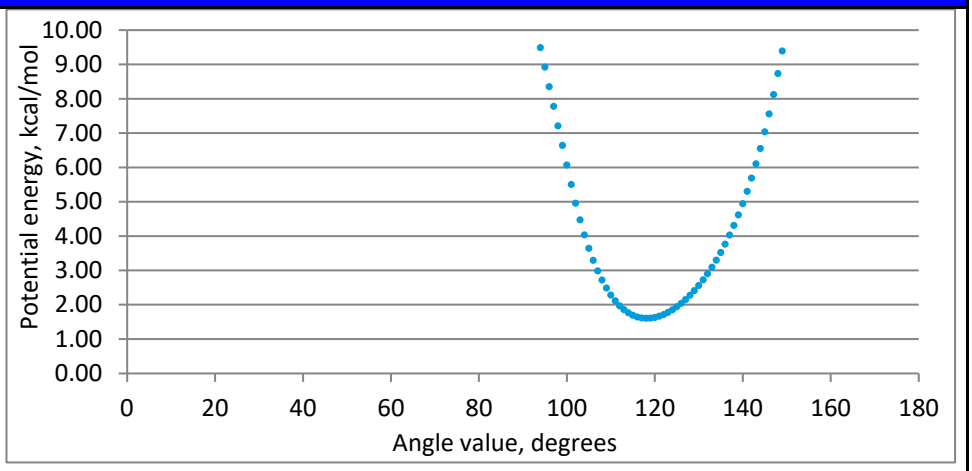

iii. Non-bonded potentials

Interaction	Potential (energy [kcal·mol^{-1}] versus distance [Å])
E···E	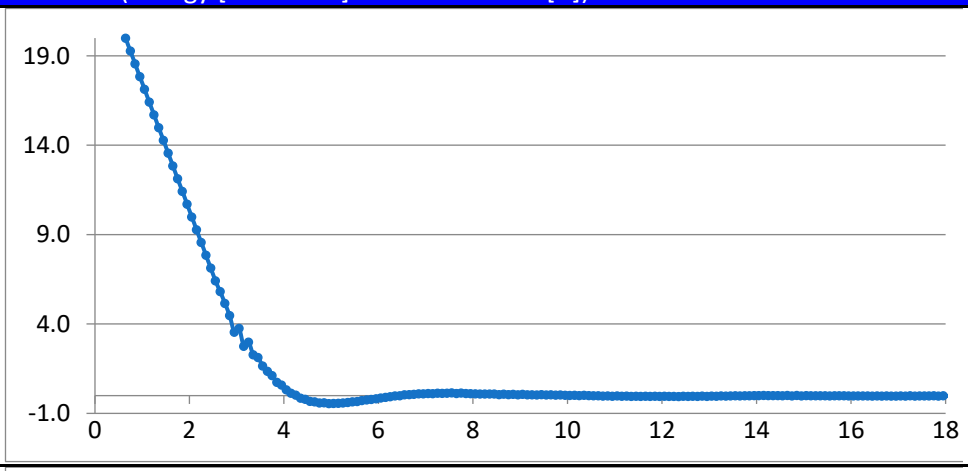
E···G	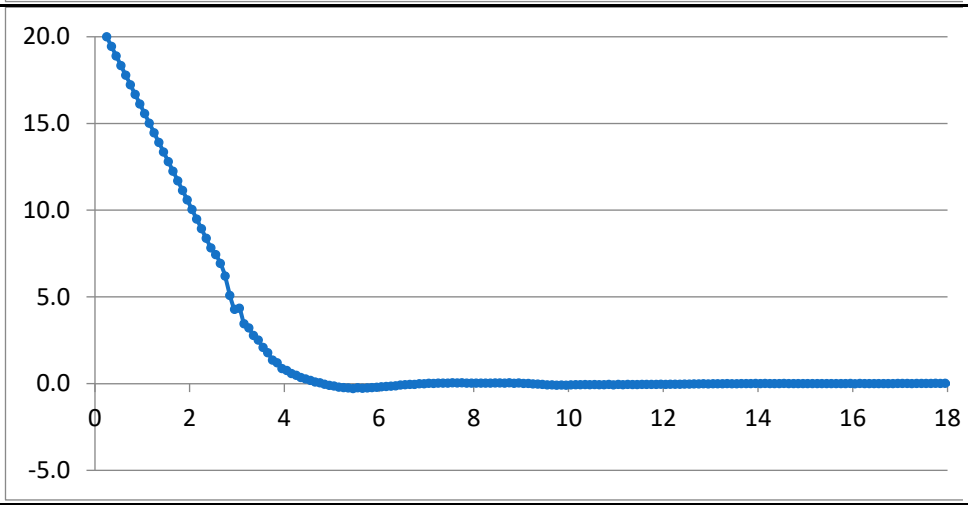

Interaction	Potential (energy [kcal·mol^{-1}] versus distance [Å])
E···B	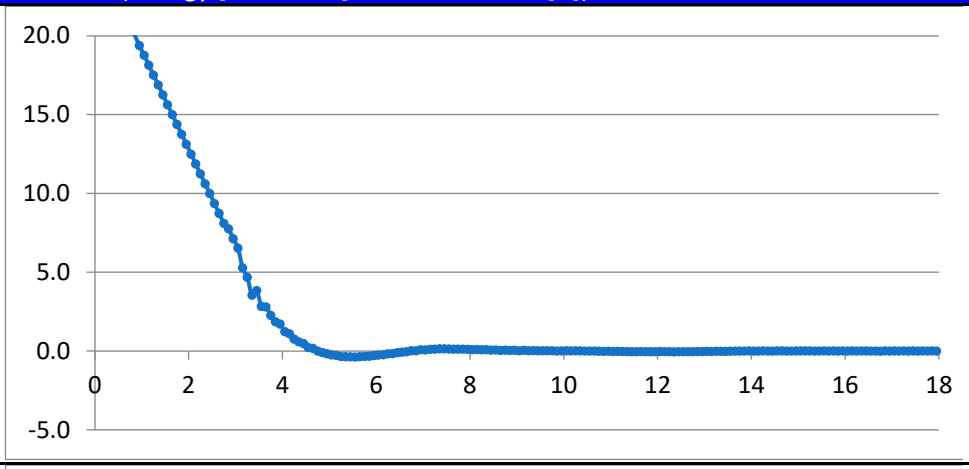
E···Ad	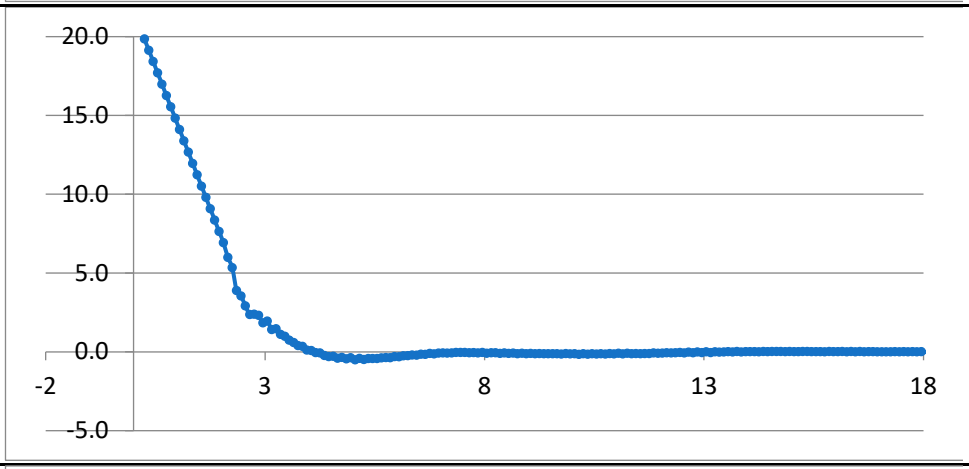
E···Ae	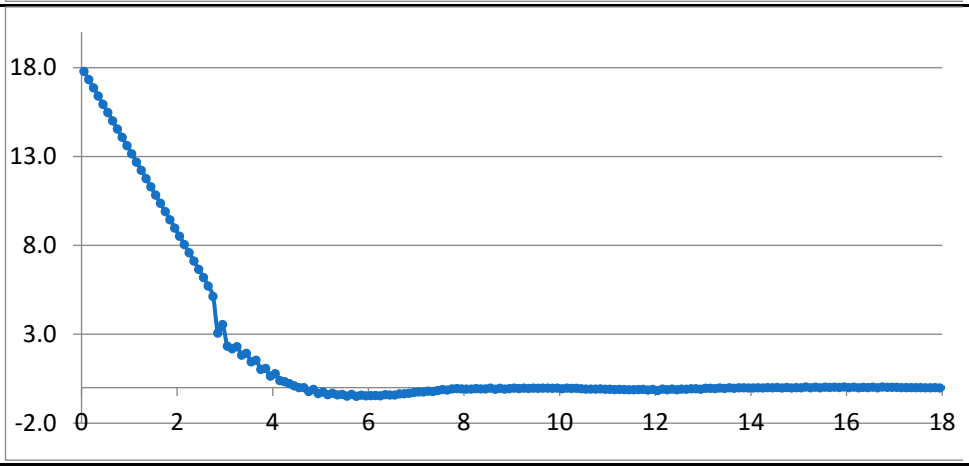

Interaction	Potential (energy [kcal·mol^{-1}] versus distance [Å])
E···Ay	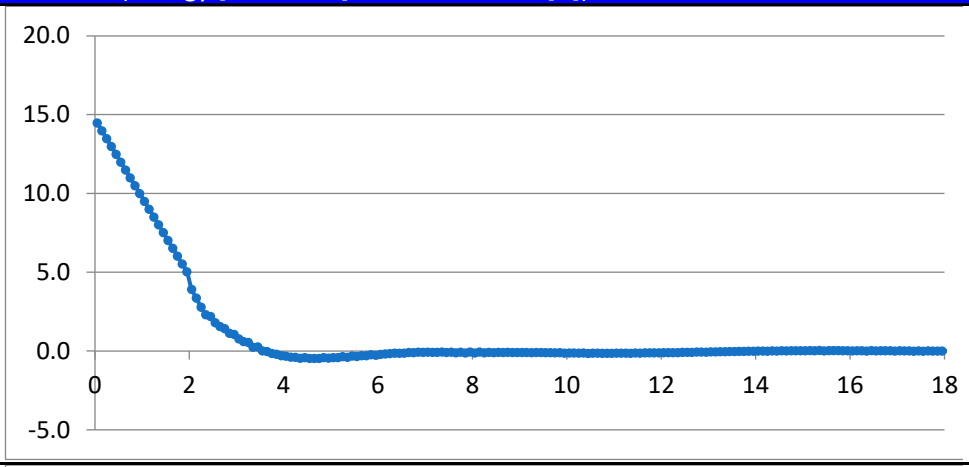
E···Y	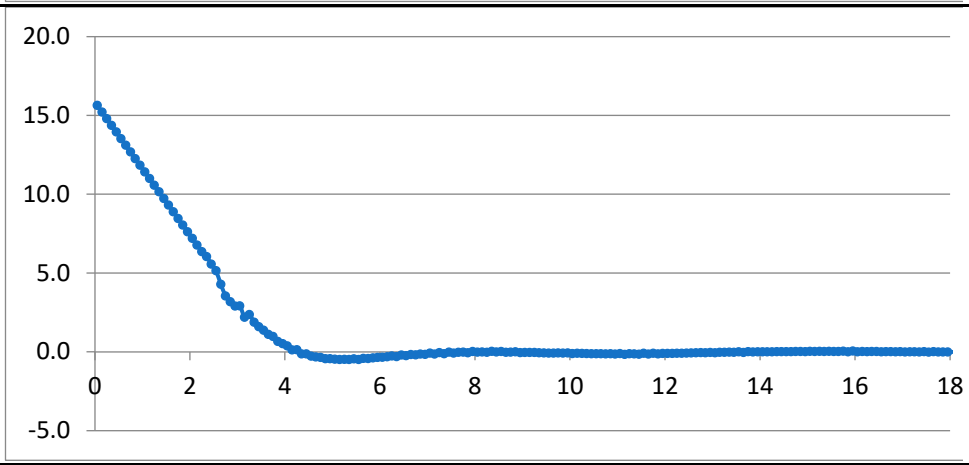
G···G	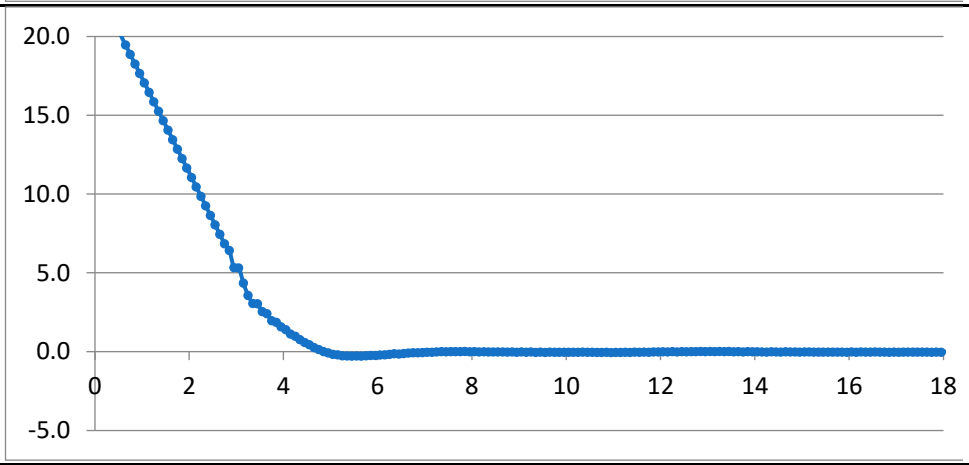

Interaction	Potential (energy [kcal·mol^{-1}] versus distance [Å])
G···B	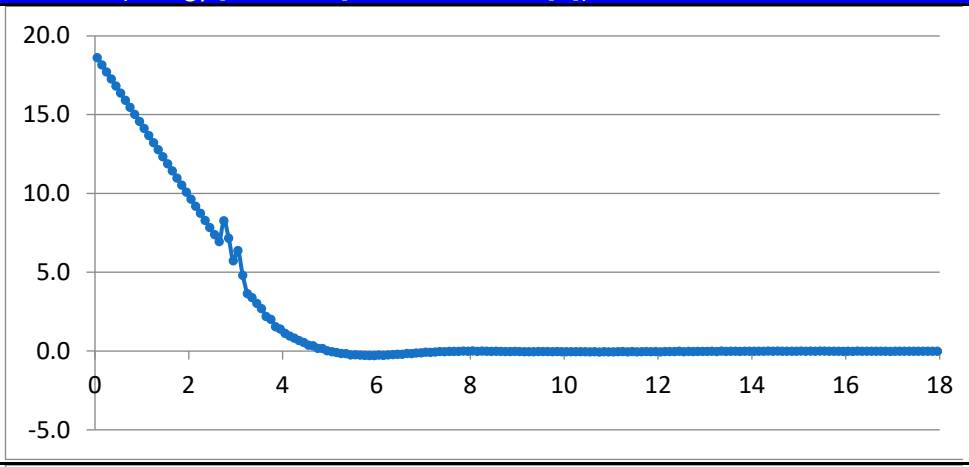
G···Ad	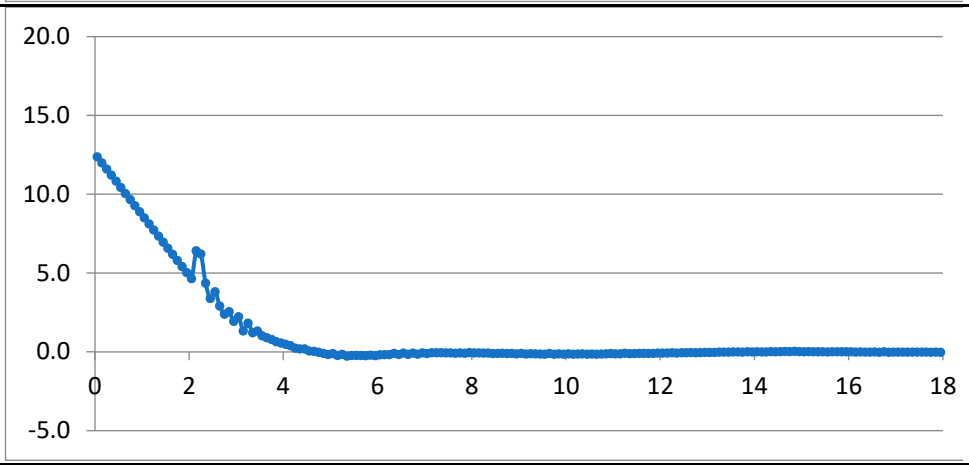
G···Ae	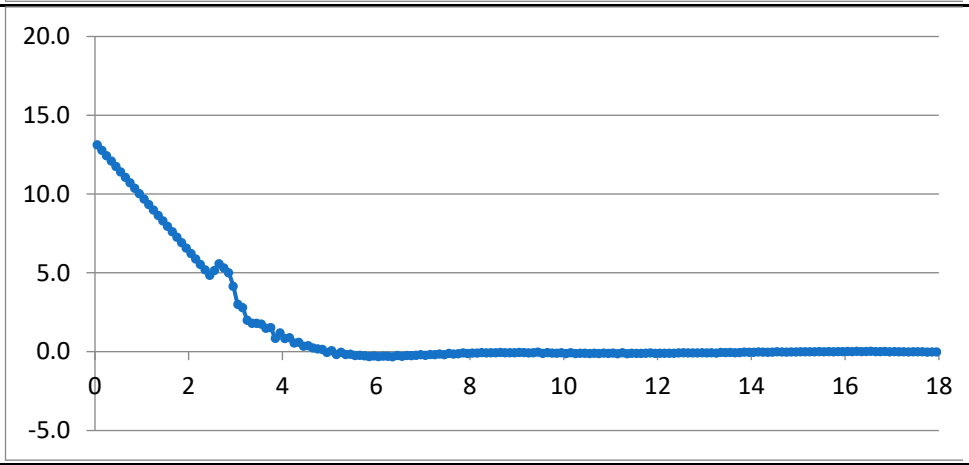

Interaction	Potential (energy [kcal·mol^{-1}] versus distance [Å])
G···Ay	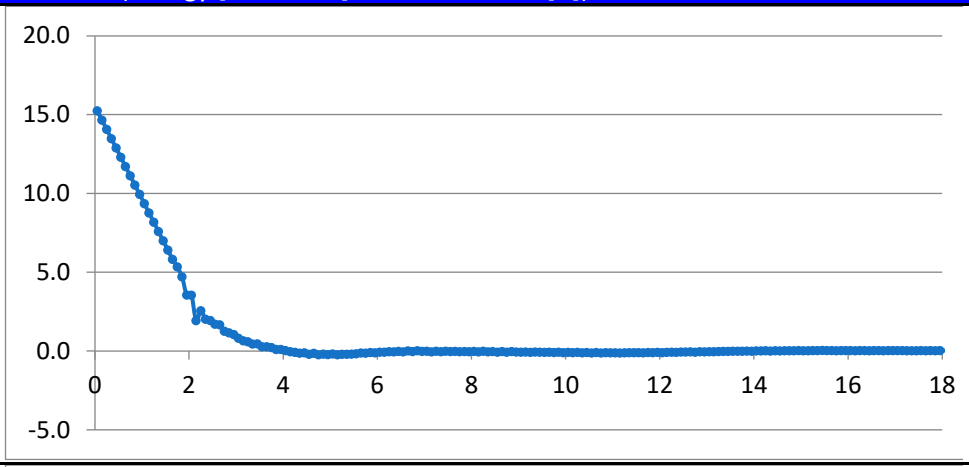
G···Y	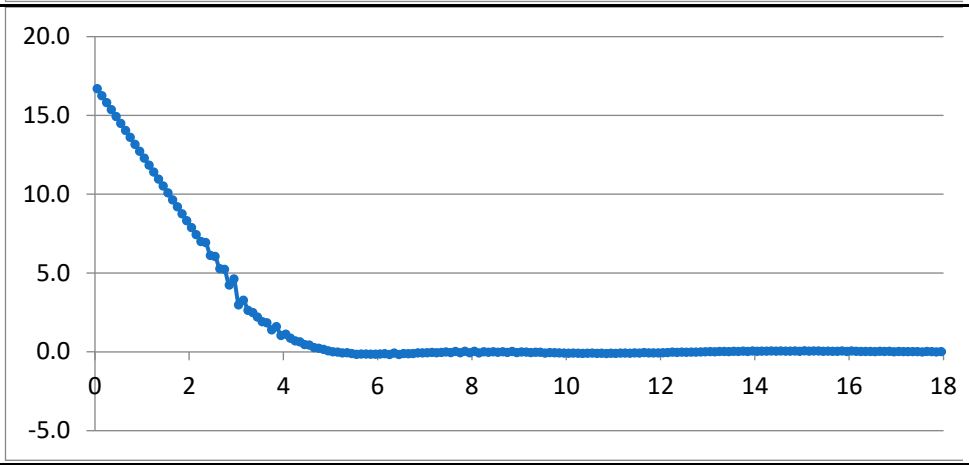
B···B	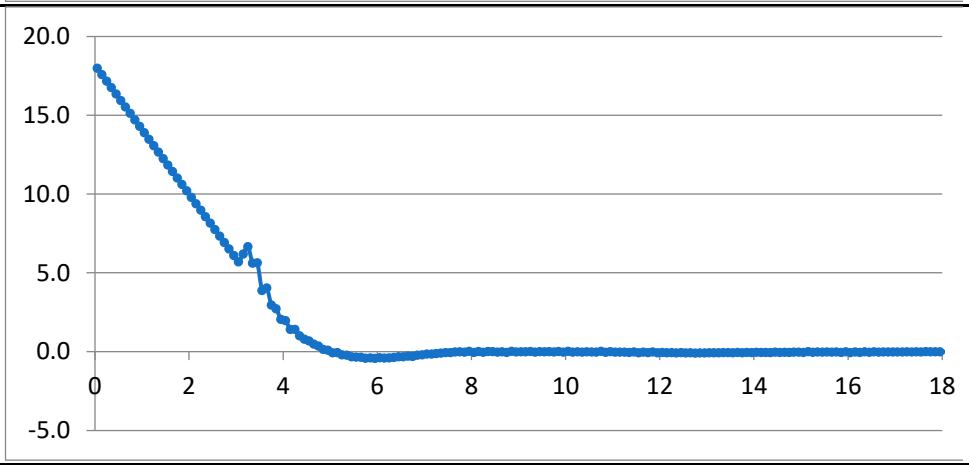

Interaction	Potential (energy [kcal·mol^{-1}] versus distance [Å])
B···Ad	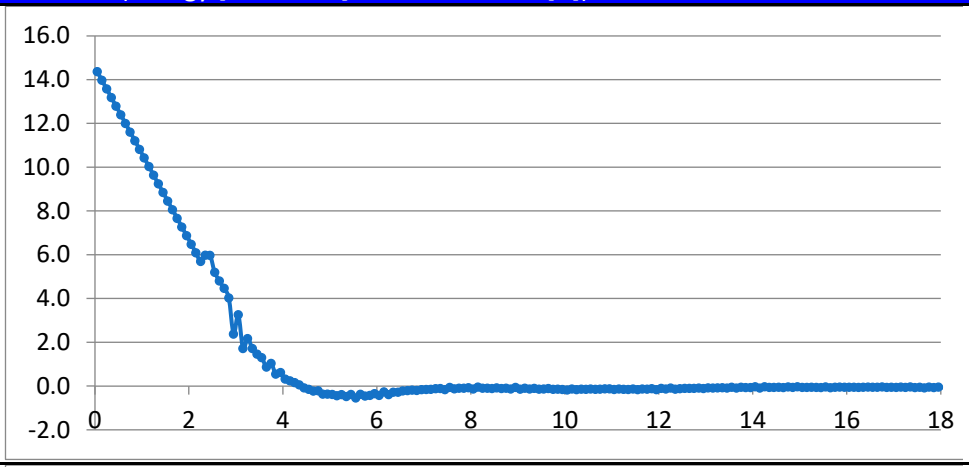
B···Ae	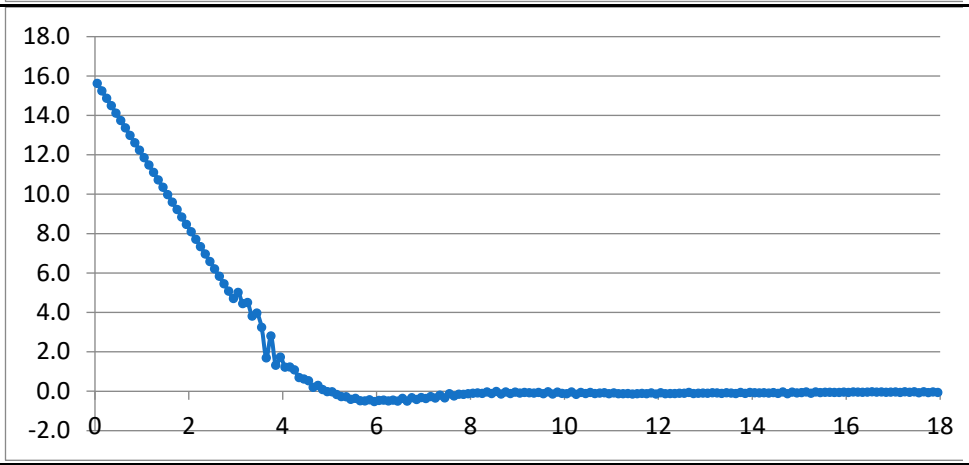
B···Ay	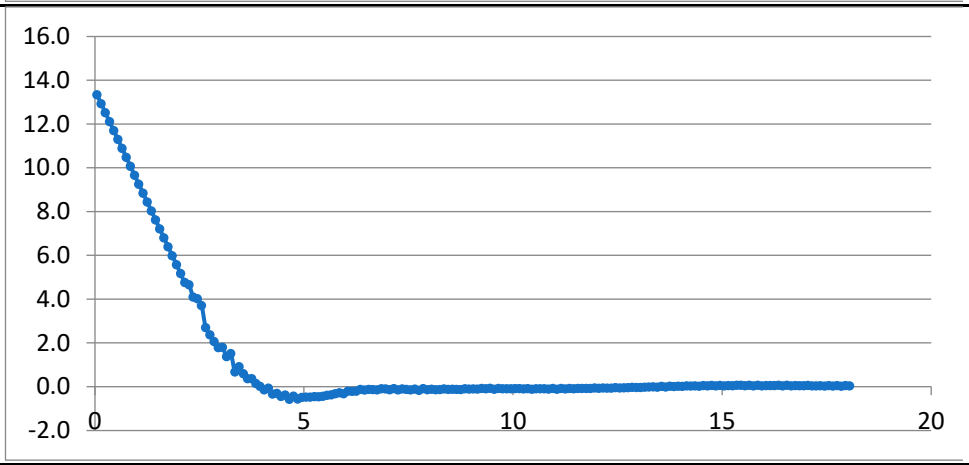

Interaction	Potential (energy [kcal·mol^{-1}] versus distance [Å])
B···Y	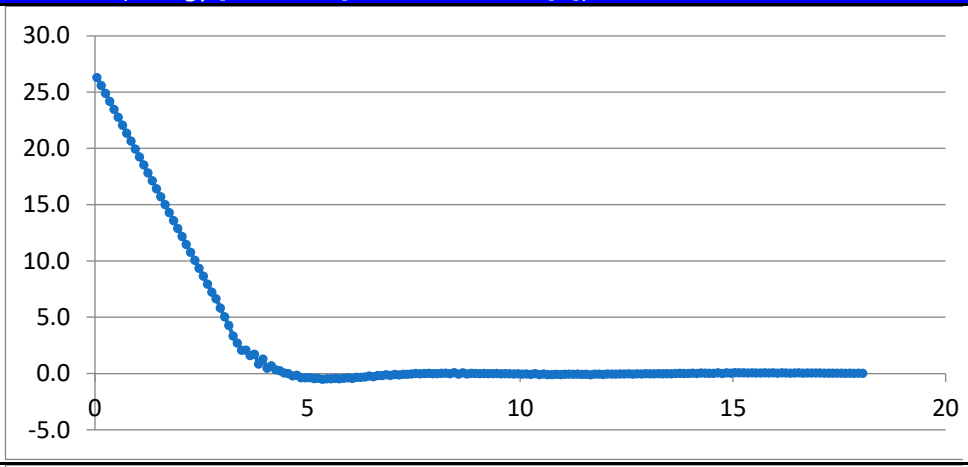
Ad···Ad	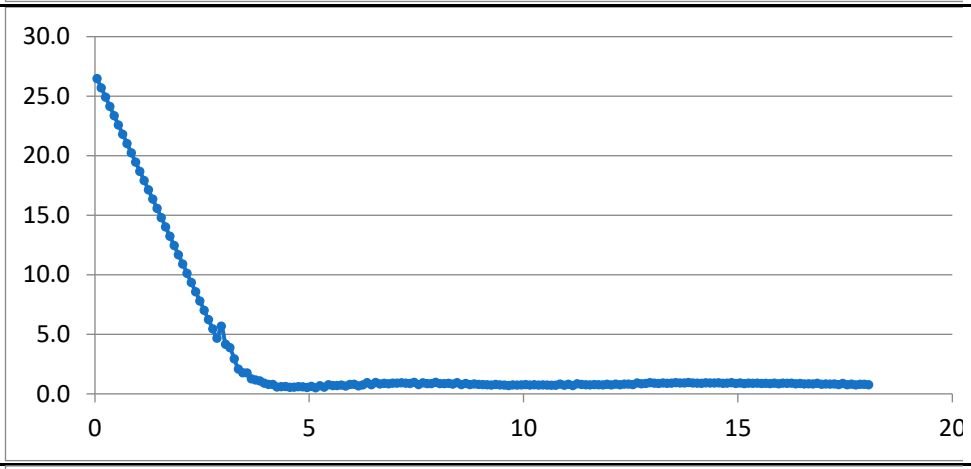
Ad···Ae	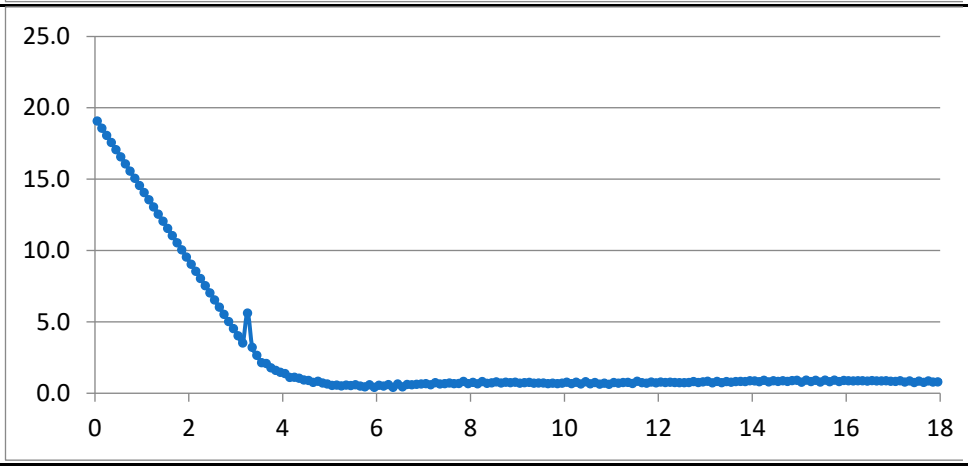

Interaction	Potential (energy [kcal·mol^{-1}] versus distance [Å])
Ad···Ay	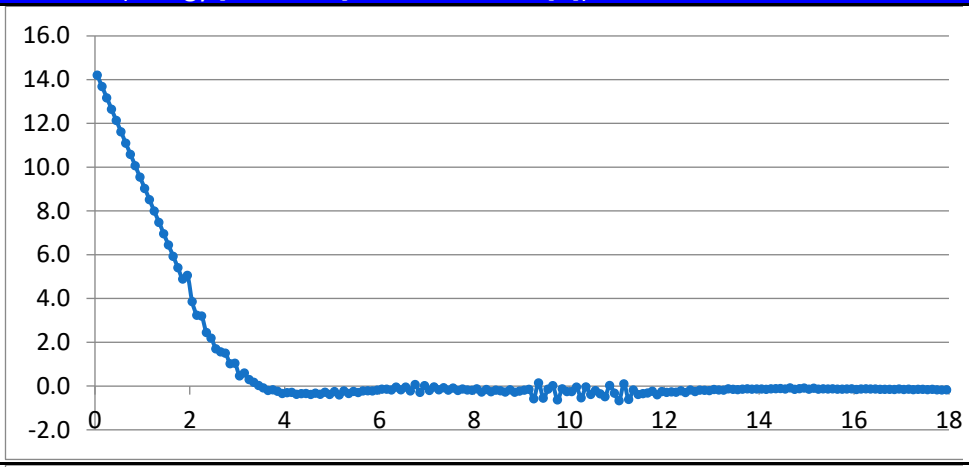
Ad···Y	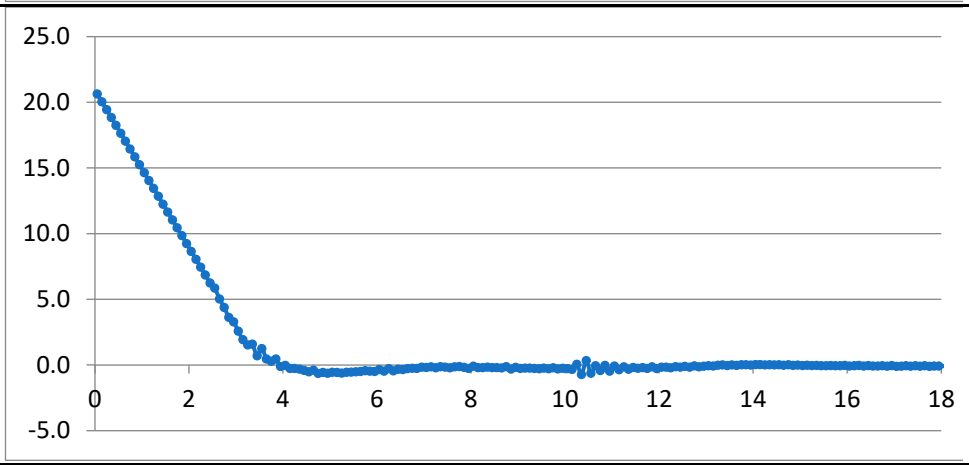
Ae···Ae	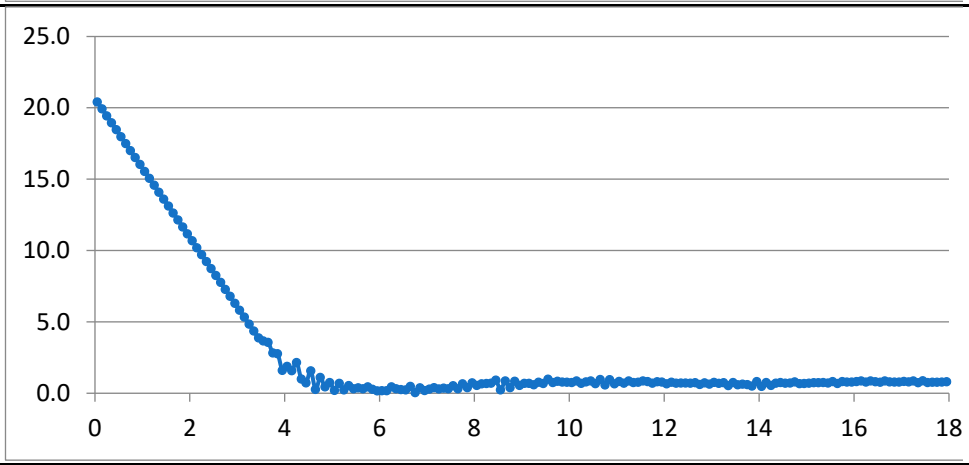

Interaction	Potential (energy [kcal·mol^{-1}] versus distance [Å])
Ae···Ay	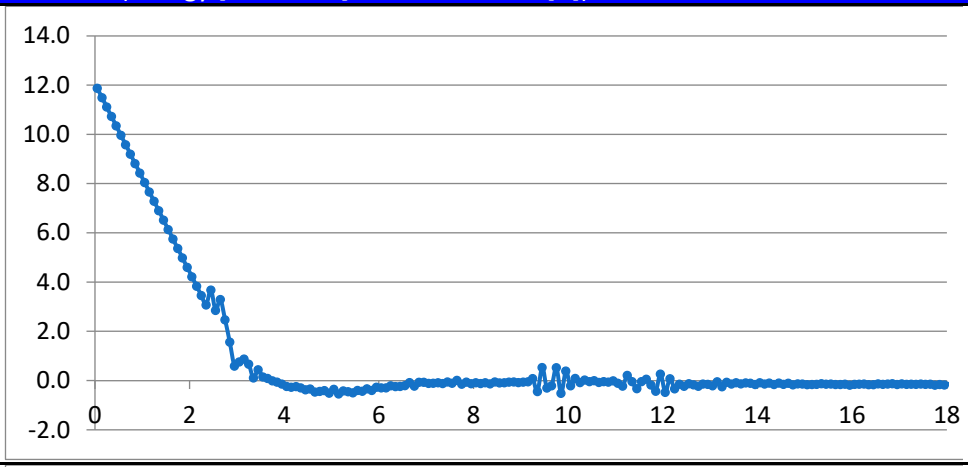
Ae···Y	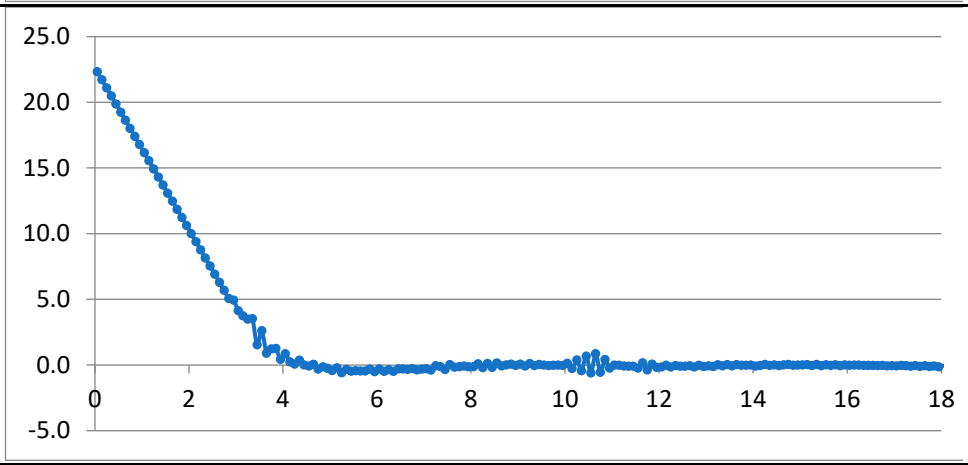
Ay···Ay	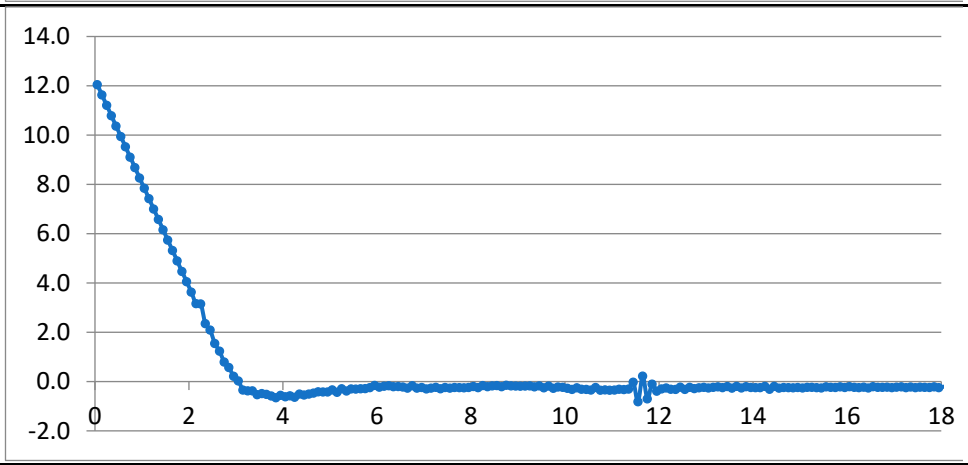

Interaction	Potential (energy [kcal·mol^{-1}] versus distance [Å])
Ay···Y	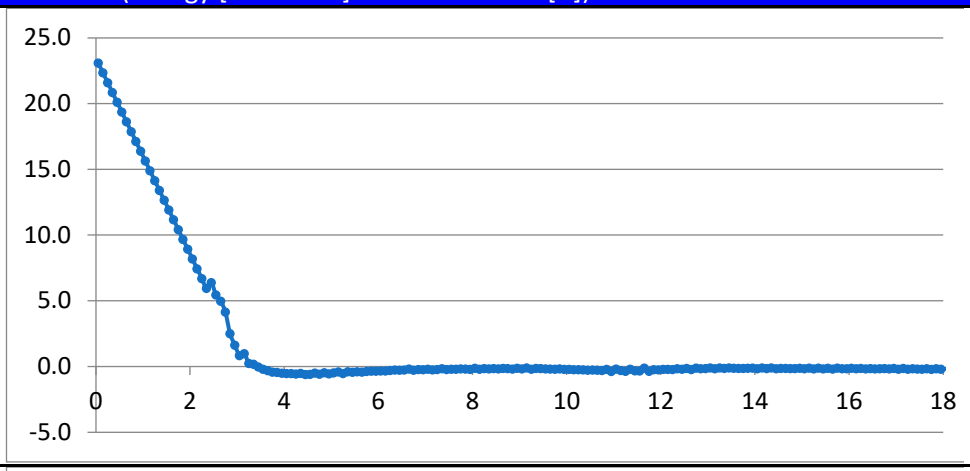
Y···Y	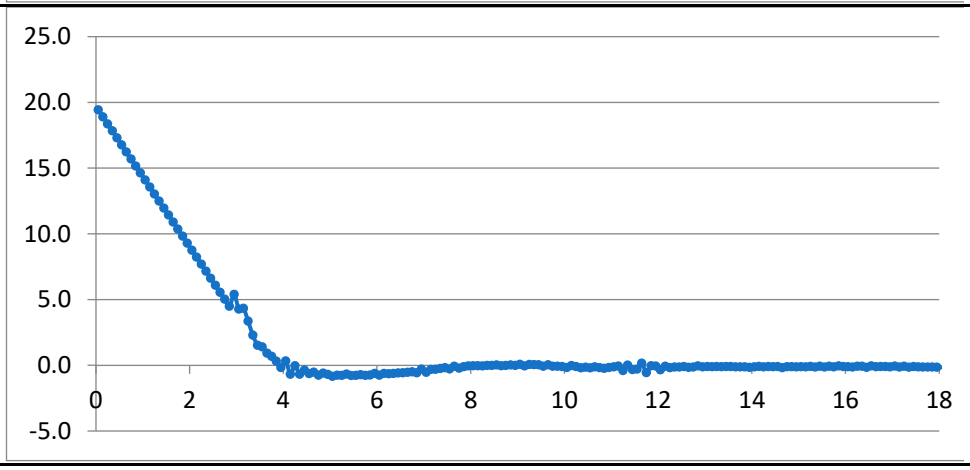

iv. Stability of developed EPO-CG force field

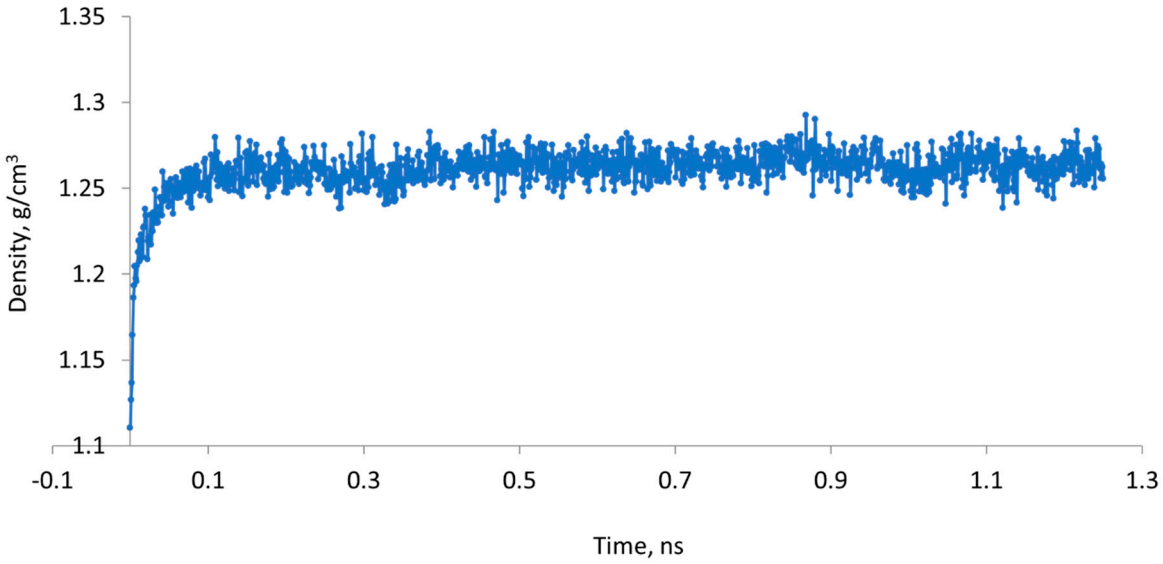

Figure S6. Density versus time in cross-linked CG epoxy system.

Supplementary Note S4: Epoxy graphene composites CG force field (EPO-GRP-CGff)

i. Non-bonded potentials

Non-bonded			
E ··· Gr	B ··· Gr	Ae ··· Gr	Y ··· Gr
G ··· Gr	Ad ··· Gr	Ay ··· Gr	

Table S5. List of potentials in the developed EPO-GRP-CGff forcefield for non-bonded interactions.

Interaction	Potential (energy [kcal·mol^{-1}] versus distance [Å])
E···Gr	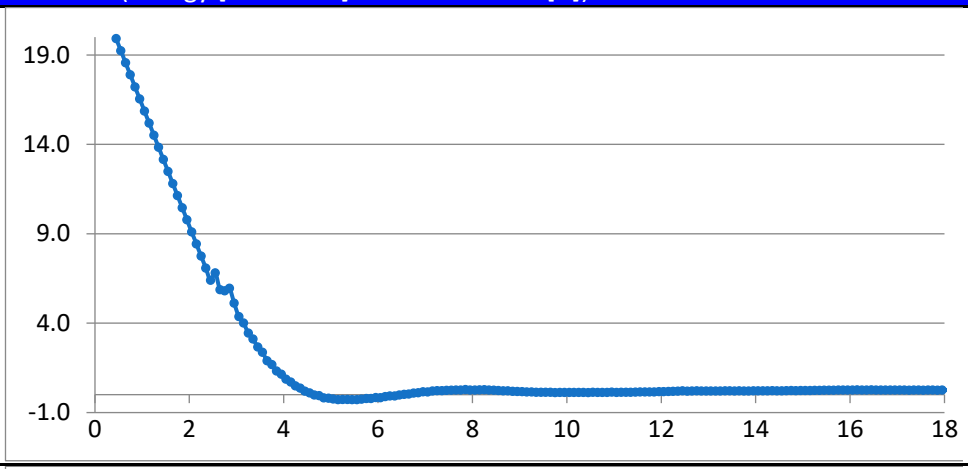
G···Gr	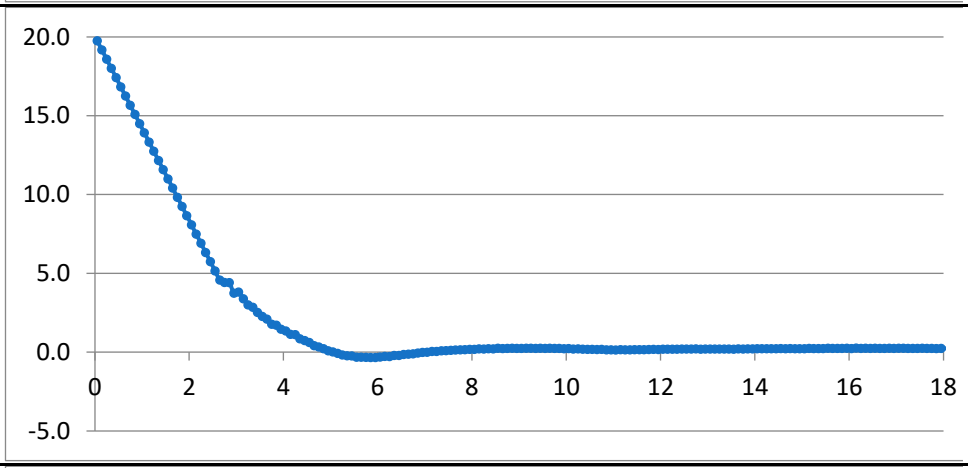
B···Gr	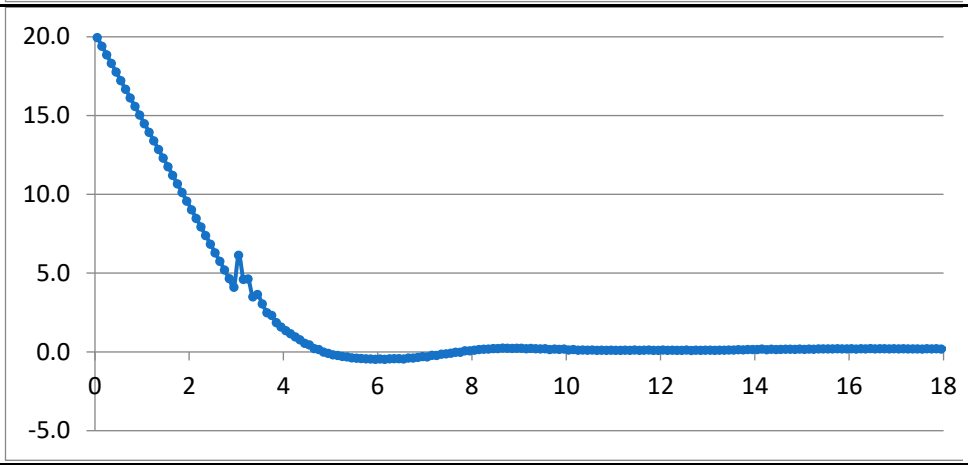

Interaction	Potential (energy [kcal·mol^{-1}] versus distance [Å])
Ad···Gr	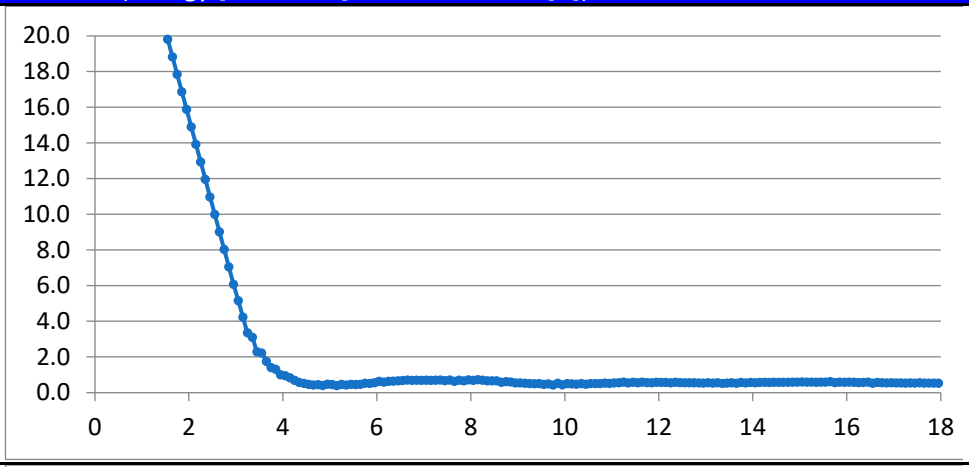
Ae···Gr	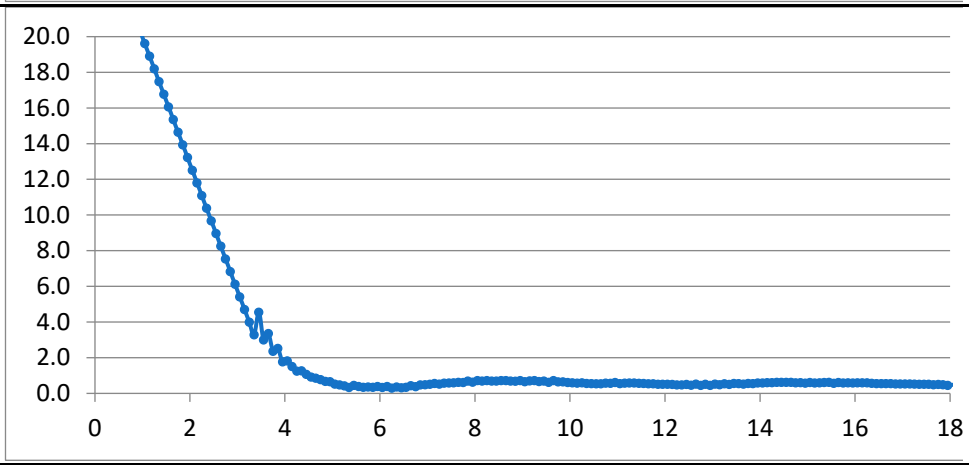
Ay···Gr	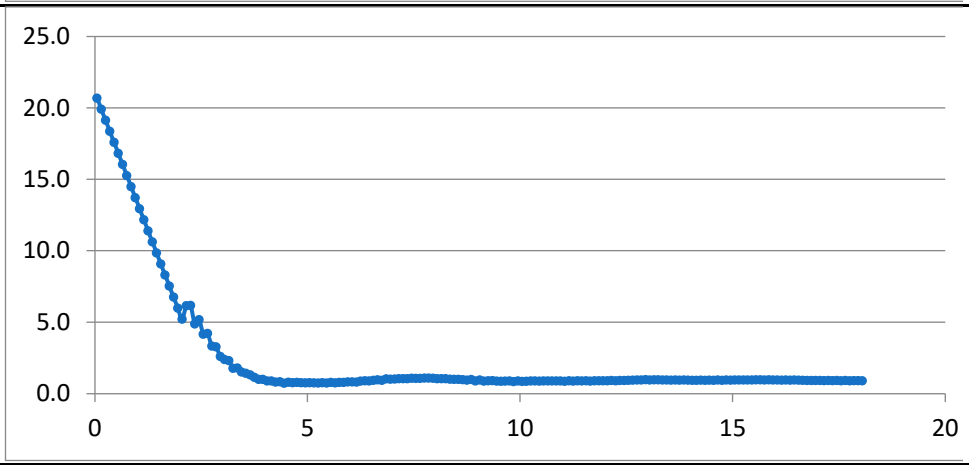

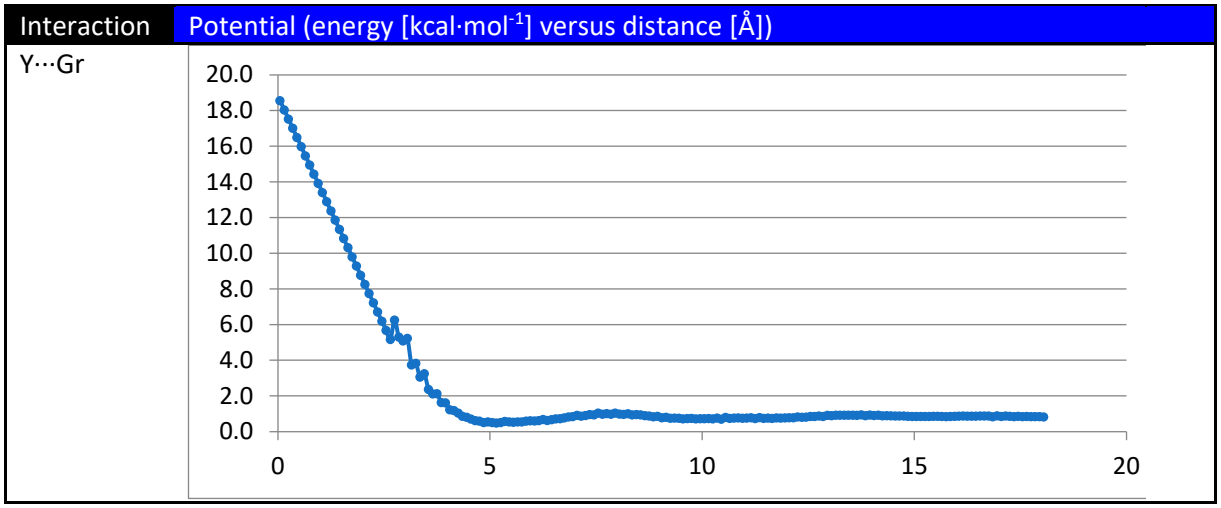

Supplementary Note S5: Tabulated results

Properties	AA MD	CG MD	Literature Ref
Density (g/cm^3)	1.155 (0.003)	1.24 (0.005)	1.07-1.20 [1]–[3]
Glass transition temperature (K)	387.87	390.40	380-390 [4]
Young's modulus (GPa)	2.999 (0.010)	1.419 (0.043)	2.5-5 [1]–[3], [5]–[8]
Poisson's ratio (-)	0.293 (0.010)	0.335 (0.012)	0.22-0.33 [2], [5], [7]
Thermal conductivity (W/m-K)	0.163 (0.005)	0.099 (0.003)	0.18-0.2 [9], [10]
Specific heat capacity (kJ/kg-K)	3.5	0.55	1.0-2.0 [11], [12]

Table S6. Comparison of thermophysical properties of pure epoxy resin obtained from all-atomistic, coarse-grained molecular dynamics and literature reference values.

Properties	CG MD	AA MD Ref	Experimental Ref
Young' modulus (GPa)	981-1009	500-1200 [13]	1000 [14], [15]
Poisson's ratio (-)	0.14-0.16	0.14-0.39 [13]	0.19 [16]
Thermal conductivity (W/m-K)	520-546	800-1000 [17]	2000-5000 [18], [19]
Specific heat capacity (kJ/kg-K)	0.526	–	0.700 [20]

Table S7. Comparison of thermophysical properties of monolayer graphene sheet obtained from coarse-grained molecular dynamics and literature experimental values.

wt.%	CG MD E (GPa)	Continuum (MF) E (GPa)	Continuum (FE) E (GPa)
0.0	1.419 (0.043)	1.419	1.419 (0.043)
0.5	1.452 (0.046)	1.442	1.436 (0.004)
0.8	1.462 (0.018)	1.461	1.453 (0.011)
1.0	1.466 (0.025)	1.464	1.459 (0.008)
1.5	1.496 (0.027)	1.497	1.490 (0.000)
2.0	1.549 (0.036)	1.530	1.519 (0.022)

Table S8. Comparison of Young's modulus obtained from coarse-grained and continuum simulations.

wt.%	CG MD Poisson's ratio (GPa)	Continuum (MF) E (GPa)	Continuum (FE) E (GPa)
0.0	0.335 (0.012)	0.335	0.335 (0.012)
0.5	0.321 (0.006)	0.333	0.333 (0.000)
0.8	0.319 (0.005)	0.332	0.332 (0.000)
1.0	0.318 (0.006)	0.332	0.332 (0.000)
1.5	0.312 (0.004)	0.330	0.331 (0.000)
2.0	0.306 (0.014)	0.329	0.330 (0.001)

Table S9. Comparison of Poisson's ratio obtained from coarse-grained and continuum simulations.

wt.%	CG MD λ (W/mK)	Continuum (MF) λ (W/mK)	Continuum (FE) λ (W/mK)
0.0	0.099 (0.003)	0.099	0.099 (0.003)
0.5	0.104 (0.003)	0.108	0.107 (0.000)
0.8	0.114 (0.002)	0.111	0.109 (0.001)
1.0	0.116 (0.001)	0.113	0.111 (0.001)
1.5	0.118 (0.001)	0.118	0.115 (0.000)
2.0	0.120 (0.002)	0.123	0.120 (0.001)

Table S10. Comparison of thermal conductivity obtained from coarse-grained and continuum simulations.

References

[1] C. Liu, W. Ning, L. Tam, and Z. Yu, "Understanding fracture behavior of epoxy-based polymer using molecular dynamics simulation," *J Mol Graph Model*, vol. 101, p. 107757, Dec. 2020, doi: 10.1016/j.jmgm.2020.107757.

[2] R. Feng and R. J. Farris, "The characterization of thermal and elastic constants for an epoxy photoresist SU8 coating," *J Mater Sci*, vol. 37, no. 22, pp. 4793–4799, 2002, doi: 10.1023/A:1020862129948.

[3] H. Yu, O. Balogun, B. Li, T. W. Murray, and X. Zhang, "Building embedded microchannels using a single layered SU-8, and determining Young's modulus using a laser acoustic technique," *Journal of Micromechanics and Microengineering*, vol. 14, no. 11, pp. 1576–1584, Nov. 2004, doi: 10.1088/0960-1317/14/11/020.

[4] A. Gavrielides, T. Duguet, M. Aufray, and C. Lacaze-Dufaure, "Model of the DGEBA-EDA Epoxy Polymer: Experiments and Simulation Using Classical Molecular Dynamics," *Int J Polym Sci*, vol. 2019, pp. 1–9, Feb. 2019, doi: 10.1155/2019/9604714.

[5] A. T. Al-Halhouli, I. Kampen, T. Krah, and S. Büttgenbach, "Nanoindentation testing of SU-8 photoresist mechanical properties," *Microelectron Eng*, vol. 85, no. 5–6, pp. 942–944, May 2008, doi: 10.1016/j.mee.2008.01.033.

[6] H. Lorenz, M. Laudon, and P. Renaud, "Mechanical characterization of a new high-aspect-ratio near UV-photoresist," *Microelectron Eng*, vol. 41–42, pp. 371–374, Mar. 1998, doi: 10.1016/S0167-9317(98)00086-0.

[7] F. E. H. Tay, J. A. van Kan, F. Watt, and W. O. Choong, “A novel micro-machining method for the fabrication of thick-film SU-8 embedded micro-channels,” *Journal of Micromechanics and Microengineering*, vol. 11, no. 1, pp. 27–32, Jan. 2001, doi: 10.1088/0960-1317/11/1/305.

[8] J. Hammacher, A. Fuelle, J. Flaemig, J. Saupe, B. Loechel, and J. Grimm, “Stress engineering and mechanical properties of SU-8-layers for mechanical applications,” *Microsystem Technologies*, vol. 14, no. 9–11, pp. 1515–1523, Oct. 2008, doi: 10.1007/s00542-007-0534-7.

[9] Z. Wang *et al.*, “Dielectric properties and thermal conductivity of epoxy composites using core/shell structured Si/SiO2/Polydopamine,” *Compos B Eng*, vol. 140, pp. 83–90, May 2018, doi: 10.1016/j.compositesb.2017.12.004.

[10] J. Ren *et al.*, “Enhanced thermal conductivity of epoxy composites by introducing graphene@boron nitride nanosheets hybrid nanoparticles,” *Mater Des*, vol. 191, p. 108663, Jun. 2020, doi: 10.1016/j.matdes.2020.108663.

[11] A. C. Ackermann, M. Fischer, A. Wick, S. Carosella, B. L. Fox, and P. Middendorf, “Mechanical, Thermal and Electrical Properties of Epoxy Nanocomposites with Amine-Functionalized Reduced Graphene Oxide via Plasma Treatment,” *Journal of Composites Science*, vol. 6, no. 6, p. 153, May 2022, doi: 10.3390/jcs6060153.

[12] X. Wang, Q. Wang, L. Gao, and Y. Jia, “Effects of key thermophysical properties on the curing uniformity of carbon fiber reinforced resin composites,” *e-Polymers*, vol. 18, no. 1, pp. 19–26, Jan. 2018, doi: 10.1515/epoly-2017-0104.

[13] S. Thomas, K. M. Ajith, S. U. Lee, and M. C. Valsakumar, “Assessment of the mechanical properties of monolayer graphene using the energy and strain-fluctuation methods,” *RSC Adv*, vol. 8, no. 48, pp. 27283–27292, 2018, doi: 10.1039/C8RA02967A.

[14] C. Lee, X. Wei, J. W. Kysar, and J. Hone, “Measurement of the Elastic Properties and Intrinsic Strength of Monolayer Graphene,” *Science (1979)*, vol. 321, no. 5887, pp. 385–388, Jul. 2008, doi: 10.1126/science.1157996.

[15] Q. Cao *et al.*, “A Review of Current Development of Graphene Mechanics,” *Crystals (Basel)*, vol. 8, no. 9, p. 357, Sep. 2018, doi: 10.3390/cryst8090357.

[16] A. Politano and G. Chiarello, “Probing the Young’s modulus and Poisson’s ratio in graphene/metal interfaces and graphite: a comparative study,” *Nano Res*, vol. 8, no. 6, pp. 1847–1856, Jun. 2015, doi: 10.1007/s12274-014-0691-9.

[17] L. Wang and H. Sun, “Thermal conductivity of silicon and carbon hybrid monolayers: a molecular dynamics study,” *J Mol Model*, vol. 18, no. 11, pp. 4811–4818, Nov. 2012, doi: 10.1007/s00894-012-1482-4.

[18] A. A. Balandin, “Thermal properties of graphene and nanostructured carbon materials,” *Nat Mater*, vol. 10, no. 8, pp. 569–581, Aug. 2011, doi: 10.1038/nmat3064.

[19] S. Chen *et al.*, “Thermal conductivity of isotopically modified graphene,” *Nat Mater*, vol. 11, no. 3, pp. 203–207, Mar. 2012, doi: 10.1038/nmat3207.

[20] Q.-Y. Li *et al.*, “Measurement of specific heat and thermal conductivity of supported and suspended graphene by a comprehensive Raman optothermal method,” *Nanoscale*, vol. 9, no. 30, pp. 10784–10793, 2017, doi: 10.1039/C7NR01695F.